Available online at www.sciencedirect.com
SCIENCE DIRECT®
Geochimica et Cosmochimica Acta 70 (2006) 622–639
Geochimica
www.elsevier.com/locate/gca

Iron isotope fractionation during microbially stimulated Fe(II) oxidation and Fe(III) precipitation

Nurgul Balci [a,f], Thomas D. Bullen [b], Kerstin Witte-Lien [c], Wayne C. Shanks [d], Mikael Motelica [e], Kevin W. Mandernack [a,*]

[a] Department of Chemistry and Geochemistry, Colorado School of Mines, 1500 Illinois Street, Golden, CO 80401, USA
[b] Water Resources Discipline, U. S. Geological Survey, Menlo Park, CA 94025, USA
[c] Department of Geology and Geological Engineering, Colorado School of Mines, Golden, CO 80401, USA
[d] Geologic Discipline, U. S. Geological Survey, Denver, CO 80225, USA
[e] Bureau Recherche Geologique et Minieres, Orleans, France
[f] Department of Geology, Istanbul Technical University, Turkey

Received 7 February 2005; accepted in revised form 26 September 2005

Abstract

Interpretation of the origins of iron-bearing minerals preserved in modern and ancient rocks based on measured iron isotope ratios depends on our ability to distinguish between biological and non-biological iron isotope fractionation processes. In this study, we compared $^{56}Fe/^{54}Fe$ ratios of coexisting aqueous iron ($Fe(II)_{aq}$, $Fe(III)_{aq}$) and iron oxyhydroxide precipitates ($Fe(III)_{ppt}$) resulting from the oxidation of ferrous iron under experimental conditions at low pH (<3). Experiments were carried out using both pure cultures of *Acidothiobacillus ferrooxidans* and sterile controls to assess possible biological overprinting of non-biological fractionation, and both SO_4^{2-} and Cl^- salts as Fe(II) sources to determine possible ionic/speciation effects that may be associated with oxidation/precipitation reactions. In addition, a series of ferric iron precipitation experiments were performed at pH ranging from 1.9 to 3.5 to determine if different precipitation rates cause differences in the isotopic composition of the iron oxyhydroxides. During microbially stimulated Fe(II) oxidation in both the sulfate and chloride systems, $^{56}Fe/^{54}Fe$ ratios of residual $Fe(II)_{aq}$ sampled in a time series evolved along an apparent Rayleigh trend characterized by a fractionation factor $\alpha_{Fe(III)aq-Fe(II)aq} \sim 1.0022$. This fractionation factor was significantly less than that measured in our sterile control experiments (~1.0034) and that predicted for isotopic equilibrium between $Fe(II)_{aq}$ and $Fe(III)_{aq}$ (~1.0029), and thus might be interpreted to reflect a biological isotope effect. However, in our biological experiments the measured difference in $^{56}Fe/^{54}Fe$ ratios between $Fe(III)_{aq}$, isolated as a solid by the addition of NaOH to the final solution at each time point under N_2-atmosphere, and $Fe(II)_{aq}$ was in most cases and on average close to 2.9‰ ($\alpha_{Fe(III)aq-Fe(II)aq} \sim 1.0029$), consistent with isotopic equilibrium between $Fe(II)_{aq}$ and $Fe(III)_{aq}$. The ferric iron precipitation experiments revealed that $^{56}Fe/^{54}Fe$ ratios of $Fe(III)_{aq}$ were generally equal to or greater than those of $Fe(III)_{ppt}$, and isotopic fractionation between these phases decreased with increasing precipitation rate and decreasing grain size. Considered together, the data confirm that the iron isotope variations observed in our microbial experiments are primarily controlled by non-biological equilibrium and kinetic factors, a result that aids our ability to interpret present-day iron cycling processes but further complicates our ability to use iron isotopes alone to identify biological processing in the rock record.

1. Introduction

Iron transformations in freshwater, marine, and soil environments are often coupled to the cycling of carbon, nitrogen, sulfur, and oxygen (Ghiorse, 1984; Nealson et al., 1988; Ehrlich, 1996). Ferric iron (Fe(III)) oxyhydroxides, the common solid products of ferrous iron (Fe(II)) oxidation, serve as important electron acceptors for the anaerobic decomposition of organic carbon in many aquatic and terrestrial environments (Lovley and Phillips, 1986a,b, 1987; Glasauer et al., 2003; Kappler et al.,

* Corresponding author.
E-mail address: kmandern@mines.edu (K.W. Mandernack).

0016-7037/$ - see front matter © 2005 Elsevier Inc. All rights reserved.
doi:10.1016/j.gca.2005.09.025

2004). Understanding processes of Fe(II) oxidation is important because Fe(III) oxyhydroxides scavenge trace metals in aquatic environments such as acid mine drainage (AMD) and thus strongly influence their fate and transport (Bigham et al., 1990; Ferris et al., 1989; Blowes et al., 2003; Jambor, 2003). In oxygenated, low pH (<3) environments, Fe(II) oxidation is largely mediated by bacteria due to slower reaction rates of abiotic oxidation mechanisms (Lizama and Suzuki, 1989; Schwertmann and Fitzpatrick, 1992; Nordstrom and Southam, 1997; Savic et al., 1998; Morgan and Stumm, 1998). Fe(II) oxidation at low pH is often mediated by *Acidothiobacillus* and *Leptosprillum* bacteria that are commonly found in AMD (Nordstrom and Southam, 1997; Schrenk et al., 1998; Brett and Banfield, 2003). Conversely, Fe(II) oxidation often proceeds abiotically in oxygenated environments at higher pH (Schwertmann and Fitzpatrick, 1992).

Biological and chemical oxidation of Fe(II) aqueous species ($Fe(II)_{aq}$) to Fe(III) aqueous species ($Fe(III)_{aq}$) and Fe(III) precipitates ($Fe(III)_{ppt}$) proceeds through a variety of pathways depending on the particular geochemistry of the system. Following oxidation of $Fe(II)_{aq}$, various $Fe(III)_{aq}$ complexes may form [e.g., $Fe(OH)_3$, $Fe_2(CO_3)_3$, $Fe_2(SO_4)_3$, and $FeCl_3$] depending on pH and ligand concentrations (Jambor, 2003). Subsequent precipitation of different $Fe(III)_{ppt}$ minerals will be influenced by concentrations of these $Fe(III)_{aq}$ complexes (Bigham et al., 1990). In addition, different biological and/or chemical oxidation pathways may leave unique iron isotope "fingerprints" on the resulting $Fe(III)_{ppt}$ pool. Therefore, $\delta^{56}Fe$ values (defined as the per mil difference of $^{56}Fe/^{54}Fe$ of a sample relative to that of a standard material) of the solids may be a useful tool for tracing the geochemical conditions and/or biological influences controlling Fe(II) oxidation (Beard et al., 2003; Anbar, 2004; Croal et al., 2004).

Recent studies have suggested that metabolic processes, which include multiple enzymatic oxidation steps, can produce significant isotopic fractionation of iron. For example, Beard et al. (1999) observed that during microbial reduction of Fe(III) in ferrihydrite by *Shewanella algae*, $\delta^{56}Fe$ of the product $Fe(II)_{aq}$ was ~1.3‰ less than that of the remaining ferrihydrite substrate. Similarly, Croal et al. (2004) observed that during oxidation of $Fe(II)_{aq}$ by anaerobic, photoautotrophic bacteria, $\delta^{56}Fe$ of $Fe(II)_{aq}$ was ~1.5‰ less than that of the product $Fe(III)_{ppt}$. These observations led to the hypothesis that $\delta^{56}Fe$ values of iron oxide, oxyhydroxide, and carbonate minerals in sedimentary rocks, ferromanganese nodules, and Precambrian banded iron formation, with values of $\delta^{56}Fe$ ranging from −1.6 to 0.9‰ when compared to terrestrial igneous rocks, could be due to biological fractionation (Beard et al., 1999, 2003). However, Mandernack et al. (1999) observed no significant iron isotope fractionation between either $Fe(II)_{aq}$ or $Fe(III)_{aq}$ and magnetite produced intracellularly by two different strains of magnetotactic bacteria, one of which was grown in replicate under micro-aerophilic and anaerobic conditions with different iron salts. In this latter study of non-metabolic magnetite synthesis, the authors proposed that binding of iron to the cell wall constituted the rate-limiting step of the overall process, resulting in total consumption of the bound iron during intracellular magnetite synthesis and thus no opportunity for significant iron isotope fractionation.

Several recent studies have shown that abiotic chemical reactions can produce significant fractionation of iron isotopes (e.g., Anbar et al., 2000; Matthews et al., 2001; Johnson et al., 2002; Skulan et al., 2002; Roe et al., 2003). From the theoretical perspective, Schauble et al. (2001) used published vibrational spectroscopic data and an empirical force field model to develop estimates of iron isotope fractionation between coexisting aqueous iron species. For the Fe-hexaquo complexes, they determined that $\delta^{56}Fe$ of $[Fe(III)(H_2O)_6]^{3+}$ should be 5.4‰ greater than that of coexisting $[Fe(II)(H_2O)_6]^{2+}$ at 25 °C. In a subsequent study, Anbar et al. (2005) used a refined theoretical approach (density functional theory) to demonstrate that $\delta^{56}Fe$ of $[Fe(III)(H_2O)_6]^{3+}$ should be ~3‰ greater than that of coexisting $[Fe(II)(H_2O)_6]^{2+}$. This latter value is similar to the range of $\delta^{56}Fe$ observed in natural materials (e.g., Beard and Johnson, 2004), and thus the variations in nature might be controlled wholly or in part by abiotic processes.

From the experimental perspective, Bullen et al. (2001) used a pH-buffered reactor apparatus under batch and flow-through (i.e., steady-state) conditions to study the isotopic consequences of abiotic oxidation of $Fe(II)_{aq}$ and accompanying precipitation of ferrihydrite under O_2-rich conditions at circum-neutral pH. In these experiments, and in a parallel field investigation of ferrihydrite precipitation from CO_2-charged spring waters, the product $Fe(III)_{ppt}$ was observed to have $\delta^{56}Fe$ 1–2‰ greater than that of coexisting $Fe(II)_{aq}$. Bullen et al. (2001) proposed that the extent of isotopic fractionation could depend on the complexation of Fe(II) with various anionic ligands, and suggested that readily oxidized $[Fe(II)(H_2O)_{6-x}(OH)_x]^{(2-x)+}$ aqueous species may have greater $\delta^{56}Fe$ than bulk $Fe(II)_{aq}$. Thus, the resulting mineral product of oxidation could carry the relatively heavy isotopic signature of these reactive Fe(II) aqueous species or their reaction intermediates. Subsequently, Johnson et al. (2002) and Welch et al. (2003) conducted isotope exchange experiments using mixtures of pure Fe(II) and Fe(III) aqueous solutions having similar $\delta^{56}Fe$ values. These studies demonstrated that at 22 ± 2 °C, $\delta^{56}Fe$ of $[Fe(III)(H_2O)_6]^{3+}$ in the mixtures was ~2.9‰ greater than that of coexisting $[Fe(II)(H_2O)_6]^{2+}$, a result attributed to equilibrium isotope effects accomplished through electron transfer. An additional important contribution of these studies, based on exchange experiments using isotopically enriched iron, was the demonstration that isotopic equilibration between $[Fe(III)(H_2O)_6]^{3+}$ and $[Fe(II)(H_2O)_6]^{2+}$ is rapid. Johnson et al. (2002) modeled the electron transfer process leading to isotopic equilibrium as a second-order reaction having a rate constant of ~0.2 s^{-1}. They further

proposed that the fractionation between $Fe(III)_{ppt}$ and $Fe(II)_{aq}$ pools observed in the Bullen et al. (2001) experiments could reflect equilibrium between the $Fe(II)_{aq}$ and $Fe(III)_{aq}$ pools overprinted by kinetic isotope effects expressed during formation of the $Fe(III)_{ppt}$ pool.

Based on these previous studies, it is clear that biological and chemical processes can produce similar magnitudes of iron isotope fractionation between coexisting iron pools in aqueous systems. Thus, our ability to determine whether biological and/or chemical reactions have contributed to iron isotope fractionation observed in the geologic record remains equivocal and controversial. An important aspect of iron isotope geochemistry that has not been addressed to date, and which is likely to provide considerable insight into variations observed in the geologic record, is the significance of redox processes at low pH (i.e., pH < 3). Low-pH environments provide ideal experimental conditions to test the ability of various processes to fractionate iron isotopes. Experiments at low pH are particularly attractive due to the general sluggishness of many (but not all) non-biological reactions, broad co-stability of Fe(II) and Fe(III) aqueous species, and availability of numerous acidophilic bacteria that stimulate iron redox processes.

To address this gap in our understanding, we conducted a series of biological and non-biological experiments under controlled laboratory conditions at low pH. The aim of these experiments was to elucidate the causes of isotopic fractionation between coexisting $Fe(II)_{aq}$ and $Fe(III)_{aq}$ pools. This experimental work is a critical part of a larger study of iron redox and cycling processes in natural acid mine drainage settings. We determined the $\delta^{56}Fe$ values of coexisting $Fe(II)_{aq}$, $Fe(III)_{aq}$, and $Fe(III)_{ppt}$ formed as a result of Fe(II) oxidation at pH < 3 during long-term (i.e., 6–10 weeks) experiments with *Acidothiobacillus ferrooxidans* and in abiotic controls. The ability to measure the isotopic contrast between coexisting $Fe(II)_{aq}$ and $Fe(III)_{aq}$ pools is a novel contribution, and allows more rigorous assessment of biologic controls on iron redox processes than was possible in previous studies (e.g., Beard et al., 1999; Croal et al., 2004) which necessarily focused on the iron isotope contrast between $Fe(II)_{aq}$ and ferrihydrite substrate or precipitate due to the small size of the $Fe(III)_{aq}$ pool under their study conditions. In addition, we conducted short- and long-term (i.e., 5 min vs. 2 week) Fe(III) precipitation experiments to determine the importance of kinetic isotope fractionation effects during formation of $Fe(III)_{ppt}$. Integrated assessment of reactants, reaction intermediates, and products helped to determine (1) if bacteria that stimulate the oxidation step are capable of imparting a unique iron isotope "biosignature" to the products; and (2) if the iron isotope contrast between $Fe(II)_{aq}$ and $Fe(III)_{ppt}$ is determined by fractionation accompanying the oxidation step, by equilibrium exchange between Fe(II) and Fe(III) aqueous species, by speciation of $Fe(II)_{aq}$ and $Fe(III)_{aq}$ with various anionic ligands, by kinetic effects related to Fe(III) precipitation, or by some combination of these factors.

2. Experimental design

2.1. Bacterial cultures

The acidophilic Fe(II)-oxidizing bacterium, *Acidothiobacillus ferrooxidans* (23270) (*A. ferrooxidans* formerly, *Thiobacillus ferrooxidans*), was obtained from the American Type Culture Collection (ATCC) and used in all biological experiments. Bacteria were maintained in a modified 2039-ATCC medium that contained the following concentrations per liter: 0.8 g $NH_4(SO_4)$, 2 g $MgSO_4 \cdot 7H_2O$, 0.1 g K_2HPO_4, 22 g $FeSO_4 \cdot 7H_2O$, and 5 mL Wolfe's mineral solution (1.5 g nitrilotriacetic acid, 3 g $MgSO_4 \cdot 7\ H_2O$, 0.5 g $MnSO_4 \cdot 7H_2O$, 1 g NaCl, 100 mg $FeSO_4 \cdot 7H_2O$, 100 mg $CoCl_2 \cdot 6H_2O$, 100 mg $CaCl_2$, 100 mg $ZnSO_4 \cdot 7H_2O$, 100 mg $CuSO_4 \cdot 7H_2O$, 10 mg $AlK(SO_4)_2 \cdot 12H_2O$, 10 mg H_3BO_3, and 10 mg $Na_2MoO_4 \cdot 2H_2O$ per liter). The medium was prepared by adding the above and 5 mL Wolfe's mineral solution to 795 mL de-ionized (DI) water. This salt solution was then filter-sterilized using pre-sterilized 0.2 μm cellulose acetate filters and the salt solution was adjusted to pH 2.3 with trace-metal-grade H_2SO_4 acid. $FeSO_4 \cdot 7\ H_2O$ (22 g) salt was then added to 200 mL of acidified DI water and immediately filter-sterilized. The salt medium and the Fe(II) solution were aseptically combined. *A. ferrooxidans* was subcultured three times before being grown for the iron isotope experiments.

2.2. $FeSO_4$ oxidation at 25 °C

The first set of biological experiments was carried out at 25 °C. For these experiments, 100 mL of filter-sterilized ferrous sulfate medium was added to 200 mL sterile-serum bottles inoculated with 2 mL of the *A. ferrooxidans* culture. The culture had been incubating for 10 days inside the closed serum bottles. To reduce inevitable carry-over of minor iron oxyhydroxides from the inoculating culture to the experimental solution, the bacterial inoculum was centrifuged at 1500 rpm (Donati et al., 1997; Sampson et al., 2000) and the supernatant containing the bacteria was used to inoculate the serum bottles. We note that although a small amount of iron oxyhydroxide precipitate may have carried over into the centrifuged inoculum, iron contributed to the experimental solutions as precipitate was probably insignificant relative to the amount of iron in the filter-sterilized ferrous sulfate medium used in each experiment, and probably had the same iron isotope composition. Replicate abiotic control experiments were set up using the same medium but were not inoculated with *A. ferrooxidans*.

For each set of biological experiments, four serum bottles were incubated at 25 °C for up to 6 weeks (Table 1). Due to the slower rates of chemical Fe(II) oxidation at pH < 3.0, only two serum bottles were prepared for each set of abiotic experiments. The pH of the medium was monitored throughout the experiments. At each sampling

Table 1
Chemical and Fe isotope compositions of biological and abiotic oxidation experiments using ferrous sulfate medium

Day	Pre-separation				Post-separation					δ^{56}Fe						
	pH	Fe[II] (mg)	Fe[III] (mg)	f[a]	pH[b]	Fe[II] (mg)[c]	Fe[III] (mg)[d]	Fe[II] (%)[e]	Fe[III] (%)[f]	Fe_{mix} (‰)[g]	$Fe[II]_{aq}$ (‰)[h]	$Fe[III]_{aq}$ (‰)[h]	$Fe[III]_{ppt}$ (‰)[h]	$Fe[II]_{aq}$ (‰)[i]	$Fe[III]_{aq}$ (‰)[i]	Fe_{mix} (‰)[i]
25 °C-A																
0	2.31	4670	10	1.00	—	—	—	—	—	−0.22	—	—	—		—	—
7	2.31	3490	930	0.75	6.10	3130	130	90	86	−0.35°	−1.40°	2. 05°	2.82°	−1.58	3.68	−0.47
14	2.16	3200	1180	0.68	6.10	2910	180	91	85	−0.38°	−1.10°	1. 49°	1.55°	−1.29	2.30	−0.32
28	2.21	2660	1370	0.57	6.10	2640	250	99	82	−0.60°	−1.40°	1. 80°	1.70°	−1.71	1.86	−0.49
42	2.11	2390	2090	0.51	5.60	2350	20	98	99	−0.30°	−1.39°	1. 03°	0.68°	−1.41	1.08	−0.25
25 °C-B																
0	2.30	4300	100	0.98	—	—	—	—	—	−0.20°	—	—	—		—	—
7	2.41	3580	820	0.81	5.60	3260	85	92	90	−0.20°	−0.60°	1. 14°	0.25°	−0.66	1.92	−0.18
14	2.35	2960	1390	0.67	5.10	2740	30	93	98	−0.25°	−1.10°	1. 27°	0.44°	−1.13	1.66	−0.24
28	2.31	2540	1690	0.58	5.00	2200	50	90	97	−0.26°	−1.20°	0. 91°	0.88°	−1.25	1.36	−0.21
42	2.29	820	2520	0.19	4.90	720	60	88	98	−0.36°	−3.70°	0. 58°	0.36°	−4.06	.77	−0.42
4 °C																
0	2.40	4435	85	0.98	—	—	—	—	—	−0.20°	—	—	—		—	—
28	2.81	3650	1100	0.81	5.60	3140	80	86	93	−0.20°	−1.05°	1. 59°	2.90°	−1.14	2.95	−0.19
42	2.92	3180	1540	0.70	5.55	2990	190	94	94	−0.20°	−0.88°	1. 21°	0.78°	−1.02	1.52	−0.19
56	3.32	2950	2110	0.65	5.20	2800	130	95	94	−0.24°	−1.35°	1. 33°	0.43°	−1.48	1.54	−0.22
70	3.03	2430	1750	0.54	5.40	2190	10	90	99	−0.20°	−1.58°	0. 79°	1.65°	−1.59	1.12	−0.46
25 °C-abiotic																
0	2.30	4250	15	0.99	—	—	—	—	—	−0.18[s]	—	—	—		—	—
14	2.35	4051	200	0.95	4.20	4054	6	100	97	−0.34[s]	−0. 38[s]	1.75[s]	1.85[s]	−0. 38	1.75	−0.28
42	2.29	3800	360	0.89	4.20	3795	5	100	99	−0.31[s]	−0.55[s]	1.13[s]	1.29[s]	−0.55	1.13	−0.40

Dash indicates values not determined. Superscripts on measured Fe isotope values indicate technique: o, Orleans Neptune multi-collector ICPMS; s, UC Santa Cruz Neptune multi-collector ICPMS.
[a] Proportion Fe[II] remaining.
[b] pH used in the separation experiments.
[c,d] Concentration after separation.
[e,f] Percent recovery during separation.
[g] Measured value of mixture used for separation.
[h] Measured values.
[i] Calculated values based on mass balance (calculated $\delta^{56}Fe[II]_{aq}$ and $\delta^{56}Fe[III]_{aq}$ determined by simultaneously solving isotope mass balance equations describing each sampled fraction).

point (7, 14, 28, and 42 days) during the incubation period, one serum bottle was filtered using 0.1 μm cellulose acetate filters under aseptic conditions. The filtered precipitate and an aliquot of the filtrate were frozen and later analyzed for Fe isotopic compositions. Total iron and $Fe(II)_{aq}$ concentrations in the culture medium were measured using a DR/700 Hach colorimeter at each sampling point (Table 1). $Fe(III)_{aq}$ concentrations were calculated as the difference between total iron and $Fe(II)_{aq}$. In order to separately measure the δ^{56}Fe values of both $Fe(II)_{aq}$ and $Fe(III)_{aq}$, a method was developed for the chemical separation of $Fe(III)_{aq}$ from each product solution, as discussed in detail below.

2.3. $FeSO_4$ oxidation at 4 °C

Biological experiments with $FeSO_4$ medium were carried out at 4 °C (environmental room) in order to determine possible temperature effects on bacterial Fe(II) oxidation rates and resulting iron isotope compositions. The composition of the medium used in these experiments was identical to that in the $FeSO_4$ experiments conducted at 25 °C. One hundred milliliters of filter-sterilized ferrous sulfate medium, which had previously been refrigerated at 4 °C, was added to 200 mL sterile-serum bottles inoculated with 2 mL of the *A. ferrooxidans* culture, which was also kept at 4 °C in the environmental room overnight. Abiotic control experiments were set up using the same medium but were not inoculated. For each set of biological experiments, four serum bottles were incubated at 4 °C for up to 10 weeks. Because chemical Fe(II) oxidation is slower, only two serum bottles were prepared for each set of abiotic experiments. The pH of the medium was monitored over the period of the experiments. At each sampling point (28, 42, 56, and 70 days) during the incubation period, one serum bottle was filtered using 0.1 μm cellulose acetate filters and the filtered precipitate and an aliquot of the filtrate were frozen. The measurements of total iron and Fe(II) concentrations in the culture medium, as well as the Fe(II)/Fe(III) separation experiments, were carried out at 4 °C in the environmental room. All experimental solutions used for the measurements and separation experiments

(e.g., NaOH and DI water) were equilibrated at 4 °C before use in the experiments.

2.4. $FeCl_2$ oxidation at 25 °C

To observe possible speciation effects on biological iron isotope fractionation resulting from possible anionic ligand interactions with $Fe(II)_{aq}$ and/or $Fe(III)_{aq}$, a second set of experiments were carried out using a $FeCl_2$ medium at 25 °C. For these experiments, 6 g of $FeCl_2$ replaced the ferrous sulfate in the 2039 medium and the Wolfe's mineral solution was made using ferrous chloride instead of ferrous sulfate. In this case, 1 L of modified medium contained: 0.6 g $NH_4(Cl)$; 0.1 g K_2HPO_4; 1.59 g $MgCl_2 \cdot 6\,H_2O$; ~6 g of $FeCl_2$; and 5 mL modified Wolfe's mineral solution (with Cl^- salt). The pH of the medium was adjusted to 2.3 using trace-metal-grade HCl. The amount of Fe(II) added was adjusted in order that chloride concentrations were kept to a minimum, as high concentrations (>5 g/L) have an inhibitory effect on *A. ferrooxidans* (Suzuki, 1999; Harahuc et al., 2000). In addition, the experiments were inoculated with bacteria that were grown in a starter medium that had been modified to minimize carry-over of sulfate. Because the bacteria grow more slowly in the chloride medium (Fry et al., 1986), this experiment ran for 77 days (Table 2). As before, abiotic control experiments were set up under the same experimental conditions.

2.5. Fe(II)/Fe(III) separation experiments

To measure the δ^{56}Fe values of $Fe(II)_{aq}$ and $Fe(III)_{aq}$ that coexist in solution at pH < 3.0, chemical methods were developed to quantitatively separate $Fe(II)_{aq}$ and $Fe(III)_{aq}$. Fifty microliter aliquots of medium were taken at each sampling point and ~0.1 mL of 10 M NaOH was added to adjust the sample to a final pH of ~5. This method forces rapid precipitation of any $Fe(III)_{aq}$ and generally results in >90% separation of $Fe(II)_{aq}$ from $Fe(III)_{aq}$. Because Fe(II) in aqueous solutions is unstable in the presence of oxygen at pH > 3 and could spontaneously oxidize, the separations were carried out in an anaerobic chamber. Prior to separation, both the sample medium and NaOH were purged with pure nitrogen gas for 30 min. The sample medium was purged directly inside the serum bottles using a pre-sterilized inline gas filter (0.2 μm) and an outlet port. After purging but before NaOH addition, solutions were kept overnight in the anaerobic chamber to equilibrate with the anaerobic atmosphere. After the addition of NaOH, the sample was filtered using 0.1 μm filters to obtain the precipitated $Fe(III)_{aq}$ and the filtrate was retained for determining the $Fe(II)_{aq}$ concentrations. Following separation procedures, the filtrate was acidified with trace-metal-grade HCl to prevent possible $Fe(II)_{aq}$ oxidation. Both the precipitate and filtrate were kept frozen for subsequent iron isotope analysis. Total iron and $Fe(II)_{aq}$ concentrations were measured colorometrically in the solutions by the *Ferrozine* method before and after separation with NaOH to determine the amount of $Fe(III)_{aq}$ and $Fe(II)_{aq}$ recovered (Tables 1 and 2). Recovery was usually between 90 and 98%. In general, better recovery for both $Fe(II)_{aq}$ and $Fe(III)_{aq}$ was obtained from the chloride solution.

2.6. Abiotic ferric iron precipitation experiments

An additional series of abiotic precipitation experiments were conducted using ferric chloride and ferric sulfate

Table 2
Chemical and Fe isotope compositions of biological and abiotic oxidation experiments using ferrous chloride medium

Day	Pre-separation				Post-separation					δ^{56}Fe						
	pH	Fe[II] (mg)	Fe[III] (mg)	f [a]	pH[b]	Fe[II] (mg)[c]	Fe[III] (mg)[d]	Fe[II] (%)[e]	Fe[III] (%)[f]	Fe_{mix} (‰)[g]	$Fe[II]_{aq}$ (‰)[h]	$Fe[III]_{aq}$ (‰)[h]	$Fe[III]_{ppt}$ (‰)[h]	$Fe[II]_{aq}$ (‰)[i]	$Fe[III]_{aq}$ (‰)[i]	Fe_{mix} (‰)[i]
25 °C																
0	2.30	2840	50	0.98	—	—	—	—	—	−0.15[s]	—	—	—		—	—
35	2.16	2120	590	0.73	4.44	2010	40	95	93	−0.27[o]	−0.51[o]	1.20[o]	0.85[o]	−0.55	1.55	−0.09
56	2.07	1890	940	0.65	5.00	1850	30	98	97	−0.27[o]	−1.15[o]	1.72[o]	1.04[o]	−1.20	1.85	−0.19
70	2.07	1715	760	0.59	4.80	1620	20	94	97	−0.45[o]	−1.25[o]	1.32[o]	1.75[o]	−1.28	1.65	−0.38
77	2.05	1830	720	0.63	4.60	1860	0	102	100	−0.40[o]	−1.10[o]	1.49[o]	1.64[o]	−1.10	1.49	−0.37
25 °C-abiotic																
0	2.00	2740	0	1.00	—	—	—	—	—	−0.13[s]	—	—	—		—	—
56	2.00	2700	40	0.99	4.20	2630	0	97	100	−0.18[s]	−0.18[s]	1.06[s]	—	−0.18	3.23	−0.13

Dash indicates value not determined. Superscripts on measured Fe isotope values indicate technique: o, Orleans Neptune multi-collector ICPMS; s, UC Santa Cruz Neptune multi-collector ICPMS.

[a] Proportion Fe[II] remaining.

[b] pH used in the separation experiments.

[c,d] Concentration after separation.

[e,f] Percent recovery during separation.

[g] Measured value of mixture used for separation.

[h] Measured values.

[i] Calculated values based on mass balance (calculated $\delta^{56}Fe[II]_{aq}$ and $\delta^{56}Fe[III]_{aq}$ determined by simultaneously solving isotope mass balance equations describing each sampled fraction).

solutions over a narrow pH range (2.2–3.5) to assess whether isotopic fractionation of $Fe(III)_{aq}$ occurs during Fe-oxyhydroxide precipitation or whether ionic speciation affects iron isotopic fractionation. This pH range covers that used in the biological experiments and mimics the range measured at many AMD sites. The initial ferric chloride solution had an Fe(III) concentration of ~1300 mg/L and the ferric sulfate solution had an initial Fe(III) concentration of ~1400 mg/L. One hundred milliliter aliquots of DI water with varying amounts of concentrated NaOH were mixed with 100 mL aliquots of the ferric solutions to achieve the appropriate pH. After mixing, solutions were allowed to stand for 5 min and then were sequentially filtered through 0.8 and 0.1 μm cellulose acetate filters (Table 5). Aliquots of the filtrates were collected along with the two precipitate fractions for analysis of iron isotopic composition. For the ferric sulfate precipitation experiments, the following final pHs were prepared: 2.54, 2.67, 2.85, 3.22, and 3.35. An anaerobic duplicate of the pH 2.85 experiment was also completed in order to determine whether the presence of dissolved oxygen might also influence iron isotope fractionation associated with Fe(III) precipitation. For the ferric chloride experiments, the following pHs were used: 2.38, 2.55, 2.89, and 3.22.

A second set of precipitation experiments were conducted using a ferric chloride solution with 60 mg/L Fe(III) and a ferric sulfate solution with 100 mg/L Fe(III) to assess whether Fe(III) concentration has an effect on iron isotope fractionation during precipitation. For the ferric sulfate solution, the following pHs were used: 2.51, 2.72, 3.24, and 3.54. For the ferric chloride solution, the following pHs were used: 2.22, 2.51, 2.76, 3.27, and 3.54. These samples were filtered using only the 0.1 μm cellulose acetate filters, as the precipitates were not coarse enough to be trapped by the 0.8 μm filter.

In addition to these short-term precipitation experiments, longer-term precipitation experiments were conducted at a single pH of 2.7 and 2.5, respectively, for ferric sulfate and ferric chloride solutions (Table 6). For these experiments, separate solutions containing 600 mg/L Fe(III) from ferric chloride and 450 mg/L Fe(III) from ferric sulfate were brought to their respective pHs and allowed to stand, in the dark (to prevent photooxidation/reduction), at room temperature for 7–14 days. Samples were taken and filtered through 0.1 μm cellulose acetate filters at 30 min, 24 h, 1 week, and 2 weeks (ferric chloride solution only). Both precipitates and filtrates were retained for isotopic analysis. At the 2-week time point, there was no precipitate in the ferric sulfate solution and thus no data are available. The pH of the solutions was taken at the time of sampling to monitor possible temporal changes.

2.7. Determination of iron isotope composition

For this study, the isotopic composition of iron was determined using "double spike" measurement techniques on two different mass spectrometric analytical platforms. Thermal ionization mass spectrometry (TIMS) was used early in the study, while multi-collector inductively coupled plasma mass spectrometry (MC-ICPMS) was used later in the study. The TIMS analysis was accomplished on a Finnigan MAT 261 adjustable collector instrument in Menlo Park, CA. The MC-ICPMS analysis was accomplished on two different Thermo-Electron "Neptune" instruments, one at BRGM in Orleans, France, and the other at the University of California at Santa Cruz. In both cases, the Neptune instruments were operated in "ion beam edge resolution" mode, in which the instrument is tuned to allow resolution of the low-mass limb of the iron ion beams from those of Ar-N,O,H ion beams at the detectors (i.e., "high-resolution" technique of Weyer and Schwieters, 2003; Arnold et al., 2004). The iron isotope data obtained for this study are presented in Tables 1, 2, 4 and 5, in which each isotopic determination is keyed to its appropriate analysis platform.

Sample preparation differed for the different analytical approaches. For the TIMS analysis, an aliquot of each experimental product (i.e., reactant solution or acid digest of filter) sufficient to provide ~1.25 μg of iron was mixed with a set amount of ^{57}Fe–^{58}Fe mixed "double spike" enriched tracer, and the mixture was allowed to homogenize overnight on a warm plate (~50 °C). The solution was then taken to dryness and re-dissolved in 1 mL of 6 N HCl. The acid solution was loaded onto a small Teflon column containing 2 mL of AG-1-X8 anion resin and then washed with 10 mL of 6 N HCl to strip other ions from the solution. Iron was then eluted from the column using 7 mL of 0.1 N HCl, and the resulting solution was taken to dryness. An amendment solution consisting of 10 μg of colloidal silica, 1 μg of alumina, and 40 μL of 0.15M H_3PO_4 was added to the iron, and the solution was again taken to dryness. The product solid was taken up in 5 μL of Teflon-distilled H_2O and loaded onto a single Re filament ribbon for mass spectrometry.

For the MC-ICPMS analysis, an aliquot of each experimental product sufficient to provide ~7 μg of iron was taken to dryness and re-dissolved in 1 mL of 7N HNO_3. The acid solution was loaded onto a small Teflon column containing 1 mL of REE-Spec resin (Eichrom Industries) and then washed with 10 mL of 7 N HNO_3 to strip other major ions from the solution. By using strong nitric acid, ferric iron and the rare earth elements are quantitatively retained on this resin, while other cations and anions are effectively separated in the wash. Iron and the rare earths were then eluted from the column using 7 mL of 0.35 N HNO_3 (i.e., 2% HNO_3, the acid strength used for the MC-ICPMS method). A 1 mL aliquot was collected from each resulting solution and measured for iron concentration on a Perkin-Elmer Elan 6000 quadrupole icpms in order to confirm quantitative recovery of iron from the column. Prior to isotopic measurement on the Neptune instruments, 1 mL of each purified solution was mixed with a set amount of the same ^{57}Fe–^{58}Fe "double spike" enriched tracer used for the TIMS analysis.

Isotopic measurements resulted in determination of the $^{56}Fe/^{54}Fe$ ratio of the sample, and used the ^{57}Fe–^{58}Fe ratio

of the sample-double spike mixture as a measure of isotopic fractionation due to mass spectrometry procedures. For the TIMS approach, individual isotopic determinations given in the data tables comprised at least 60 scans, each consisting of four 4-s measurements: a simultaneous measurement of ^{54}Fe and ^{56}Fe, a simultaneous measurement of ^{56}Fe, ^{57}Fe, and ^{58}Fe, and measurements of ^{52}Cr and ^{60}Ni in order to correct for isobaric interferences of Cr and Ni (although these corrections were generally negligible). For the MC-ICPMS approach, individual isotopic determinations given in the data tables comprised 60 scans, during which ^{54}Fe, ^{56}Fe, ^{57}Fe, and ^{58}Fe as well as ^{52}Cr and ^{60}Ni were measured simultaneously for 8 s. In both cases, the ^{56}Fe/^{54}Fe ratio of the sample was mathematically extracted from the measured composition of the sample-double spike mixture using an algorithm similar to that originally proposed by Russell et al. (1978) and employed for all isotope ratio determinations based on the double spike method at Menlo Park (e.g., Johnson et al., 2000; Bullen et al., 2001).

The isotopic data are reported here in terms of δ^{56}Fe, the per mil difference of the ^{56}Fe/^{54}Fe ratio of a sample from that of BIR-1, a U.S.G.S. basalt standard. The internal precision of an isotope composition determination is 0.15‰ or better for the TIMS method and 0.10‰ or better for the MC-ICPMS method (2σ, minimum 60 component ratio determinations). BIR-1 is used as the reference standard because (a) as an igneous rock it should have δ^{56}Fe $\sim$ 0.0‰ (cf. Beard et al., 2003); and (b) it has a complex chemical matrix that must be processed through the entire analytical procedure in order to obtain purified iron for analysis. Thus, reproducibility of its iron isotope composition provides a measure of external precision of the analytical methods. External precision on the determination of the iron isotope composition of BIR-1, analyzed throughout the mass spectrometry sessions after approximately every tenth sample measurement, was 0.11‰ for the TIMS method (2σ, $n = 20$), 0.07‰ for the MC-ICPMS method on the Neptune instrument at Orleans (2σ, $n = 9$), and 0.07‰ from the MC-ICPMS method on the Neptune instrument at Santa Cruz (2σ, $n = 25$). In addition, the iron isotope composition of the IRMM-014 iron standard was determined repeatedly throughout the mass spectrometry sessions on the Neptune instrument at Orleans, with external precision of 0.10‰ (2σ, $n = 15$). Relative to BIR-1, IRMM-014 gave δ^{56}Fe of −0.02‰, identical within analytical uncertainty to the composition of this standard relative to igneous rocks (−0.09‰) reported by Beard et al. (2003). Procedural blanks were not determined, as blank levels on filters or in reagents were assumed to be substantially less than amounts of iron in samples.

3. Results

3.1. Measured and calculated δ^{56}Fe of operational fractions

Data for the biological and abiotic oxidation experiments are presented in Table 1 (ferrous sulfate medium) and Table 2 (ferrous chloride medium). In these tables, we include both the raw data for the operational Fe(II)$_{aq}$, Fe(III)$_{aq}$, and Fe(III)$_{ppt}$ fractions (concentration and isotopic composition) and corrected data for Fe(II)$_{aq}$ and Fe(III)$_{aq}$ fractions. A correction was necessary to account for small amounts of Fe(III)$_{aq}$ remaining in solution and Fe(II)$_{aq}$ carried over into the precipitate formed during the separation of Fe(III)$_{aq}$ from the experimental solutions, respectively. The correction was accomplished by simultaneously solving the following equations describing isotope mass balance of the operational Fe(II)$_{aq}$ and Fe(III)$_{aq}$ fractions:

$$[\mathrm{Fe(II)}]_{\mathrm{Fe(II)}} \cdot \delta^{56}\mathrm{Fe(II)}_{aq} + [\mathrm{Fe(III)}]_{\mathrm{Fe(II)}} \cdot \delta^{56}\mathrm{Fe(III)}_{aq} = ([\mathrm{Fe(II)}]_{\mathrm{Fe(II)}} + [\mathrm{Fe(III)}]_{\mathrm{Fe(II)}}) \cdot \delta^{56}\mathrm{Fe(II)}_{\mathrm{aq\text{-}raw}}, \quad (1)$$

$$[\mathrm{Fe(II)}]_{\mathrm{Fe(III)}} \cdot \delta^{56}\mathrm{Fe(II)}_{aq} + [\mathrm{Fe(III)}]_{\mathrm{Fe(III)}} \cdot \delta^{56}\mathrm{Fe(III)}_{aq} = ([\mathrm{Fe(II)}]_{\mathrm{Fe(III)}} + [\mathrm{Fe(III)}]_{\mathrm{Fe(III)}}) \cdot \delta^{56}\mathrm{Fe(III)}_{\mathrm{aq\text{-}raw}}, \quad (2)$$

where $[\mathrm{Fe(II)}]_{\mathrm{Fe(II)}}$ and $[\mathrm{Fe(III)}]_{\mathrm{Fe(II)}}$ are the concentrations of Fe(II) and Fe(III) in the operational Fe(II)$_{aq}$ fraction, $[\mathrm{Fe(II)}]_{\mathrm{Fe(III)}}$ and $[\mathrm{Fe(III)}]_{\mathrm{Fe(III)}}$ are the concentrations of Fe(II) and Fe(III) in the operational Fe(III)$_{aq}$ fraction, δ^{56}Fe(II)$_{aq\text{-}raw}$ and δ^{56}Fe(III)$_{aq\text{-}raw}$ are the measured δ^{56}Fe values of the operational Fe(II)$_{aq}$ and Fe(III)$_{aq}$ fractions, and δ^{56}Fe(II)$_{aq}$ and δ^{56}Fe(III)$_{aq}$ are the calculated δ^{56}Fe values of the Fe(II)$_{aq}$ and Fe(III)$_{aq}$ components.

The robustness of this correction procedure was tested using the following mass balance calculation:

$$\delta^{56}\mathrm{Fe}_{mix} = \delta^{56}\mathrm{Fe(II)}_{aq} \cdot [\mathrm{Fe(II)}]_{aq} + \delta^{56}\mathrm{Fe(III)}_{aq} \cdot [\mathrm{Fe(III)}_{aq}, \quad (3)$$

where $[\mathrm{Fe(II)}]_{aq}$ and δ^{56}Fe(II)$_{aq}$, and $[\mathrm{Fe(III)}]_{aq}$ and δ^{56}Fe(III)$_{aq}$ are the corrected concentrations and isotope compositions, respectively, of Fe(II)$_{aq}$ and Fe(III)$_{aq}$. δ^{56}Fe$_{mix}$ is the isotopic composition of the solution containing both Fe(II)$_{aq}$ and Fe(III)$_{aq}$ prior to the separation procedure, and was measured directly (Tables 1 and 2). Using the concentration and isotopic values of the iron pools measured at each sampling point, δ^{56}Fe$_{mix}$ values were calculated using Eq. (3) and compared to the measured δ^{56}Fe$_{mix}$ values (Tables 1 and 2). Significant error in either the concentration or isotope measurements of either the pre- or post-separation aqueous or precipitate fractions would have resulted in a mismatch between the calculated and measured δ^{56}Fe$_{mix}$ values. Assuming that δ^{56}Fe of the Fe(III)$_{aq}$ pool remained constant during the precipitation process (i.e., that kinetic isotope fractionation effects between Fe(III)$_{ppt}$ and Fe(III)$_{aq}$ pools were negligible), the similarity between our measured and calculated values for δ^{56}Fe$_{mix}$ indicates that the calculated isotopic composition of the Fe(III)$_{ppt}$ pool faithfully records that of the Fe(III)$_{aq}$ pool of the experimental solution mixture. As discussed later, the assumption of negligible kinetic isotope effects during this rapid precipitation process is consistent with the results of our Fe(III) precipitation experiments in which the amount of kinetic isotope fractionation

between $Fe(III)_{ppt}$ and $Fe(III)_{aq}$ pools decreased toward zero with increasing precipitation rate.

Data for the ferric iron precipitation experiments are presented in Table 4 (short-term experiments) and Table 5 (long-term experiments). In Table 4, we include both the measured data for $\delta^{56}Fe$ of the $Fe(III)_{aq}$ and $Fe(III)_{ppt}$ fractions, as well as the calculated composition for $\delta^{56}Fe$ of the $Fe(III)_{ppt}$ fraction based on mass balance determined for the aqueous fractions using the following equation:

$$\delta^{56}Fe_{ppt} = ([Fe(III)]_{before} \cdot \delta^{56}Fe(III)_{before} - [Fe(III)]_{after} \cdot \delta^{56}Fe(III)_{after})/([Fe(III)]_{before} - [Fe(III)]_{after}), \quad (4)$$

where $Fe(III)_{before}$ and $\delta^{56}Fe_{before}$, and $Fe(III)_{after}$ and $\delta^{56}Fe_{after}$ are the iron concentrations and $\delta^{56}Fe$ values, respectively, of the aqueous fractions before and after the precipitation step, and $\delta^{56}Fe_{ppt}$ is the calculated $\delta^{56}Fe$ value of the precipitate.

3.2. Rates of Fe(II) oxidation

Oxidation of $Fe(II)_{aq}$ was observed in all experiments. *A. ferrooxidans* oxidized Fe(II) in both the ferrous sulfate and ferrous chloride media, resulting primarily in the accumulation of $Fe(III)_{aq}$ and a small amount of $Fe(III)_{ppt}$. However, because sulfate stimulates bacterial Fe(II) oxidation, the oxidation rate was greater in the experiments with sulfate medium compared to that in the experiments with chloride medium (Fig. 1). The maximum Fe(II) oxidation rate was 1.4 mM/day in the $FeSO_4$ medium and ~0.25 mM/day in the $FeCl_2$ medium. The maximum fractions of total Fe(II) oxidized were 81% (ferrous sulfate medium, 42 days) and 40% (ferrous chloride medium 77 days) (Tables 1 and 2). The amount of precipitation of ferric oxyhydroxides increased with the extent of reaction. Abiotic Fe(II) oxidation occurred in all of the non-biological experiments, but rates were much lower than in the biological experiments and in all cases less than 10% of the Fe(II) was oxidized (Tables 1 and 2). Abiotic precipitation of ferric oxyhydroxides occurred only in the $FeSO_4$ medium.

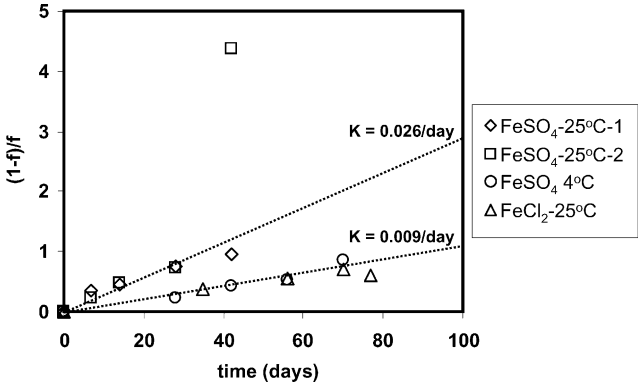

Fig. 1. Regression of data for all biological oxidation experiments, using second-order rate law (Eq. (7)) forced through a zero intercept. f is the proportion of $Fe(II)_{aq}$ remaining; the slope of the line through any given data array is equivalent to k, the reaction rate constant.

Reactions such as oxidation and isotope exchange that can be cast in terms of reaction progress are often modeled using a general rate law equation of the form:

$$df/dt = -k_n f^n, \quad (5)$$

where f is the proportion of reactant remaining after time t ($f = 1$ at $t = 0$), k is the rate constant, and n is the order of the reaction (cf. Johnson et al., 2002). In simple terms, reaction rate in a zeroth-order reaction is independent of reactant concentration, reaction rate in a first-order reaction is directly dependent on reactant concentration, reaction rate in a second-order reaction is dependent on the square of reactant concentration, and so on. Determination of reaction order can provide information on possible reaction mechanisms (e.g., simple probability for a first-order reaction, progressive reactant "poisoning" for second- and higher-order reactions), and calculated rate constants can be used to compare the relative importance of competing reactions in a complex process. For example, reaction data for isotope equilibration via electron transfer between $[Fe(II)(H_2O)_6]^{2+}$ and $[Fe(III)(H_2O)_{6-x}(OH)_x]^{(3-x)+}$ are best fit by a second-order rate law having $k = 0.18$–0.26/s (Johnson et al., 2002; Welch et al., 2003). Similarly, the reaction data for the abiotic Fe(II) oxidation experiment conducted in batch mode by Bullen et al. (2001) are best fit by a second-order rate law having $k = 0.24$/h ($r^2 = 0.98$). Thus, the electron transfer reaction proceeded ~3600 times faster than the oxidation reaction. Beard and Johnson (2004) suggested that the data for the Bullen et al. (2001) experiment is best fit by a first-order rate law, but we note that the r-squared obtained using a first-order model (0.96) is marginally worse than that obtained using the second-order model.

The most straightforward method of determining reaction order is by graphing data for reaction progress as a function of time. Integration of the general rate equation (Eq. (5)) for a given reaction order results in an expression for f in terms of t. For example, integration of Eq. (5) for a second-order reaction results in the expression

$$f = (1 + kt)^{-1}, \quad (6)$$

where k is the reaction rate constant. Eq. (6) can be recast as a simple linear function of time

$$(1 - f)/f = kt. \quad (7)$$

The data for reaction progress are then plotted graphically such that the y-axis is $(1 - f)/f$ and the x-axis is time. The r-squared value of the simple linear regression through the data is then calculated, and compared to values calculated for other reaction orders. The reaction order providing the greatest r-squared value is assumed to best describe the modeled reaction. Finally, the slope of the straight line

fitted through the data is equivalent to k, the reaction rate constant.

For all the biological oxidation experiments, reaction progress data are best fit by a second-order rate law. Treating the oxidation process as either a zeroth-order (i.e., f vs. t) or first-order (i.e., $\ln f$ vs. t) reaction results in lower r-squared values, providing support for the second-order reaction model. The data for the biological experiments are plotted in Fig. 1 in terms of a second-order rate model. Straight lines can be fitted through all data for the first 25 °C ferrous sulfate experiment, the 4 °C ferrous sulfate experiment, and the 25 °C ferrous chloride experiment. However, the data for the second 25 °C ferrous sulfate experiment are overall non-linear, due to the 42-day time point that is clearly at odds with the other data. Noting that the earlier time points for this second experiment are consistent with those of the first 25 °C ferrous sulfate experiment, we suggest that the $Fe(II)_{aq}$ concentration of the errant 42-day time point sample, which had an exceptionally low f value, was affected by an additional process not accounted for by the second-order rate mechanism. For example, it is possible that the kinetics of Fe(II) oxidation were enhanced by autocatalysis due to the large surface area on $Fe(III)_{ppt}$ at this late stage of the oxidation reaction. Disregarding this one point, the rate constant determined for both 25 °C ferrous sulfate experiments is ~0.026/day, while that for the 4 °C ferrous sulfate and 25 °C ferrous chloride experiments is ~0.009/day. The data thus demonstrate clear compositional and temperature effects on oxidation rate.

3.3. Isotopic fractionation in the biological experiments

Tables 1 and 2 give the iron isotope compositions of $Fe(II)_{aq}$, $Fe(III)_{aq}$, and $Fe(III)_{ppt}$ for the biological and abiotic oxidation experiments. Throughout the experiments, the $\delta^{56}Fe(II)_{aq}$ values are consistently lower than those of coexisting $Fe(III)_{aq}$ and $Fe(III)_{ppt}$. As shown in Fig. 2A, the data for $Fe(II)_{aq}$ in the biological experiments considered together exhibit apparent Rayleigh type behavior, which can be described by the following natural log function

$$\delta^{56}Fe(II)_{aq} = \varepsilon \ln(f), \quad (8)$$

where $\delta^{56}Fe(II)_{aq}$ is the isotopic composition of the remaining $Fe(II)_{aq}$ at a given time during the reaction; epsilon (ε) is the isotopic enrichment factor that is described by $\varepsilon = 1000(\alpha - 1)$, where $\alpha = (^{56}Fe/^{54}Fe_{Fe(III)})/(^{56}Fe/^{54}Fe_{Fe(II)})$; and f is the proportion of $Fe(II)_{aq}$ remaining after time t as defined above. If the oxidation reaction follows Rayleigh behavior, a plot of $\delta^{56}Fe(II)_{aq}$ vs. $\ln(f)$ will yield a straight line, the slope of which is equal to ε (Mariotti et al., 1981). The data for all the biological experiments plotted in Fig. 2A describe a strong linear relationship ($r^2 = 0.93$) and define a value for ε of 2.2‰, which could be interpreted to reflect an apparent Rayleigh fractionation associated with the oxidation of $Fe(II)_{aq}$ to

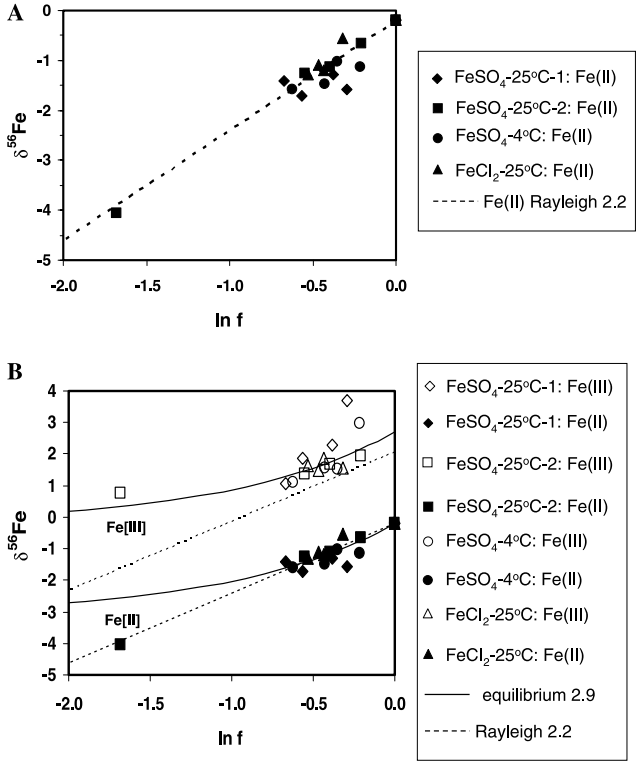

Fig. 2. $\delta^{56}Fe$ of corrected aqueous components for all biological oxidation experiments, plotted against $\ln(f)$, where f is the proportion of $Fe(II)_{aq}$ remaining. (A) Corrected $Fe(II)_{aq}$ components only, fitted with least-squares regression line having slope of 2.2 ($r^2 = 0.91$). On this log-linear plot, the slope of the regression line gives the apparent Rayleigh isotopic enrichment factor ε, which for the overall data array is 2.2‰. (B) Corrected $Fe(II)_{aq}$ and $Fe(III)_{aq}$ components, plotted in comparison to both Rayleigh fractionation (i.e., open system) trends ($\varepsilon = 2.2$‰) and equilibrium fractionation (i.e., closed system) trends ($\varepsilon = 2.9$‰).

$Fe(III)_{aq}$. A statistical analysis of this regression reveals that the slope of this line, which equals ε, falls between 1.8 and 2.7‰ at the 99% confidence interval, which is overall significantly less than the ~2.9‰ reported for isotopic equilibrium between $Fe(II)_{aq}$ and $Fe(III)_{aq}$ at low pH (Johnson et al., 2002; Welch et al., 2003), and might provide evidence of a "biological effect." In fact, simple linear regression through the three data points obtained in the abiotic ferrous sulfate oxidation experiment (Table 1) gives a value for ε of 3.4‰, consistent with isotopic equilibrium between $Fe(II)_{aq}$ and $Fe(III)_{aq}$. However, we note that although this regression appears to be robust ($r^2 = 0.97$), the uncertainty on ε is large (standard error = 0.60) due to the uncertainty on the isotopic composition of each data point and the small extent of reaction in this experiment.

However, simple Rayleigh behavior during biological oxidation is less tenable when corresponding $\delta^{56}Fe(III)_{aq}$ values are likewise considered. As shown in Fig. 2B, the $Fe(III)_{aq}$ data for all the biological experiments as a group have consistently greater $\delta^{56}Fe$ than the Rayleigh model ($\varepsilon = 2.2$‰) would predict. On the other hand, the bulk of the $Fe(II)_{aq}$ and $Fe(III)_{aq}$ data are well described by equi-

Table 3
Summary of Fe isotope fractionation among different Fe pools

Experiment	Day	f	$\Delta_{Fe[III]ppt-Fe[II]aq}$ (‰)	$\Delta_{Fe[III]aq-Fe[III]ppt}$ (‰)	$\Delta_{Fe[III]aq-Fe[II]aq}$ (‰)
Fe[II]SO_4	7	0.75	4.40	0.86	5.26
25 °C-A	14	0.68	2.84	0.75	3.59
	28	0.57	3.41	0.16	3.57
	42	0.51	2.09	0.40	2.49
Fe[II]SO_4	7	0.81	0.91	1.67	2.58
25 °C-B	14	0.67	1.57	1.22	2.79
	28	0.58	2.13	0.48	2.61
	42	0.19	4.42	0.41	4.83
Fe[II]SO_4	28	0.81	4.04	0.05	4.09
4 °C	42	0.70	1.80	0.74	2.54
	56	0.65	1.81	1.11	3.02
	70	0.54	3.24	−0.53	2.71
Fe[II]Cl_2	35	0.73	1.40	0.70	2.10
25 °C	56	0.65	2.24	0.81	3.05
	70	0.59	3.03	−0.10	2.93
	77	0.63	2.74	−0.15	2.59
Fe[II]SO_4	14	0.95	2.23	−0.10	2.13
25 °C−abiotic	42	0.91	1.84	−0.16	1.68
Fe[II]Cl_2 25 °C-abiotic	56	0.99	—	—	3.41

librium fractionation curves based on $\varepsilon = 2.9‰$. Some of the data are clearly at odds with a simple equilibrium model, particularly the 42-day time point for the second 25 °C ferrous sulfate experiment, which also is errant with respect to a simple second-order rate mechanism. However, other time points (e.g., the 7-day time point for the first 25 °C ferrous sulfate experiment; the 7-day time point for the 4 °C ferrous sulfate experiment) are displaced from the equilibrium model curves, but fit the second-order rate model curves in Fig. 1. These discrepancies apparently point to an additional process that may overprint the isotopic fractionation resulting from oxidation.

A wide range of isotopic fractionation between $Fe(III)_{aq}$ and $Fe(III)_{ppt}$ was observed in all the biological experiments. In general, the fractionation was greater in the earlier part of each experiment than in the later part, although the decrease was clearly not monotonic as each experiment progressed (Table 3). No consistent fractionation between $Fe(III)_{aq}$ and $Fe(III)_{ppt}$ was observed in the abiotic ferrous sulfate oxidation experiment. These results suggest that there is significant and complex isotopic fractionation that occurs during precipitation of the ferric oxyhydroxide solids, such that $\delta^{56}Fe$ of the operational precipitate fraction does not provide a useful surrogate of $\delta^{56}Fe(III)_{aq}$.

3.4. Abiotic Fe(III) precipitation experiments

Short- and long-term abiotic Fe(III) precipitation experiments, using ferric chloride and ferric sulfate solutions having both high and low iron concentrations, were performed to determine possible isotopic fractionation effects associated with differing rates of Fe(III)-oxyhydroxide precipitation. In these experiments, precipitation rate was varied by adjusting solution pH (i.e., lower pH resulted in slower precipitation rate). In the high-concentration experiments, various size fractions were collected (>0.8 and 0.1–0.8 μm) to determine whether precipitate grain size affected $\delta^{56}Fe$ values, which might reflect different fractionation effects during different stages of precipitation. Precipitate size also varied with the rate of precipitation, in that the larger size fraction required a greater amount of time to form. The isotopic data for all Fe(III) precipitation experiments are plotted in Fig. 3 as a function of amount of precipitate formed per reaction time, which provides an estimate of precipitation rate. We point out, however, that we did not attempt to calculate specific precipitation rates due to the difficulty of determining grain size and reactive surface area of these solids.

In all cases, precipitation resulted in solids having lesser $\delta^{56}Fe$ than that of coexisting $Fe(III)_{aq}$. In the short-term high-concentration experiments, the difference in iron isotope composition between $Fe(III)_{aq}$ and $Fe(III)_{ppt}$ (i.e., $\Delta^{56}Fe_{aq\text{-}ppt}$) decreased as precipitation rate increased in both the sulfate and chloride systems. In the short-term low-concentration experiments, decreasing $\Delta^{56}Fe_{aq\text{-}ppt}$ with increasing precipitation rate was likewise observed in the sulfate system but not in the chloride system. In the short-term high-concentration experiments, the >0.8 μm precipitate fraction displayed a greater $\Delta^{56}Fe_{aq\text{-}ppt}$ for each pH and a greater pH/rate effect than did the 0.1–0.8 μm precipitate fraction (Table 4). Considering $\delta^{56}Fe$ values of the bulk precipitate calculated by mass balance, a pH/rate effect was evident in the sulfate system that was more similar to that observed in the 0.1–0.8 μm fraction, although with different values of $\Delta^{56}Fe_{aq\text{-}ppt}$ observed for each. For the chloride system, the pH/rate effect observed in the bulk precipitate more closely approximated that observed in the

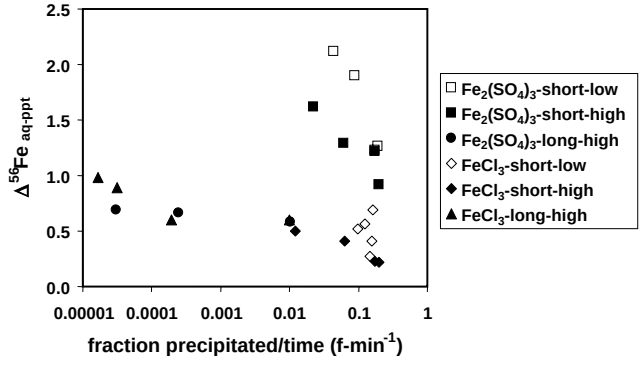

Fig. 3. Isotopic contrast ($\Delta^{56}Fe_{aq\text{-}ppt}$) between $Fe(III)_{aq}$ and $Fe(III)_{ppt}$ in ferric iron precipitation experiments, plotted as a function of fraction of precipitate formed per time of reaction (note logarithmic scale). "Short-high" and "short-low" refer to the short-term, high-concentration and low-concentration experiments, respectively; "long" refers to the long-term experiments.

Table 4
Ferric chloride and ferric sulfate precipitation experiments (short-term)

	Fe_{aq} (mg/L)	% $Fe[III]_{aq}$ remaining	$\delta^{56}Fe_{aq}$[a]	$\delta^{56}Fe_{ppt}$ (0.1–0.8 μm)[a]	$\Delta^{56}Fe_{aq\text{-}ppt}$ (0.1–0.8 μm)	$\delta^{56}Fe_{ppt}$ (>0.8 μm)[a]	$\Delta^{56}Fe_{aq\text{-}ppt}$ (>0.8 μm)	$\delta^{56}Fe_{ppt}$ (calculated)[b]	$\Delta^{56}Fe_{aq\text{-}ppt}$[c]
Fe[III]Cl₃									
pH 1.90	653	100	−0.22[m]	—	—	—	—	—	—
2.38	614	94	−0.19[m]	−0.45[s]	0.26	−0.80[m]	0.61	−0.69	0.50
2.55	444	68	−0.09[m]	−0.20[s]	0.11	−0.50[m]	0.41	−0.50	0.41
2.89	78	12	−0.02[m]	−0.05[s]	0.03	−0.28[m]	0.26	−0.25	0.23
3.22	7	1	0.00[m]	−0.06[s]	0.06	−0.24[m]	0.24	−0.22	0.22
1.90	75	100	−0.18[s]	—	—	—	—	—	—
2.22	39	51	0.03[s]	−0.22[s]	0.25	—	—	−0.49	0.52
2.51	29	39	0.12[s]	−0.18[s]	0.30	—	—	−0.44	0.56
2.76	20	27	−0.02[s]	−0.22[s]	0.20	—	—	−0.29	0.27
3.27	16	21	0.10[s]	−0.13[s]	0.23	—	—	−0.31	0.41
3.53	13.5	18	0.35[s]	−0.12[s]	0.47	—	—	−0.34	0.69
Fe[III]₂(SO₄)₃									
pH 1.90	715	100	−0.20[o]	—	—	—	—	—	—
2.54	640	89	−0.03[m]	−0.51[m]	0.48	−1.13[m]	1.10	−1.65	1.62
2.54	634	89	−0.02[o]	−0.49[o]	0.47	—	—	−1.61	1.59
2.67	493	69	0.20[o]	0.08[s]	0.12	−0.91[o]	1.11	−1.09	1.29
2.85	91	13	0.82[o]	0.45[s]	0.37	−0.15[o]	0.97	−0.34	1.16
2.86	95	13	0.90[m]	0.60[m]	0.30	−0.20[m]	1.10	−0.37	1.27
3.22	5.7	1	0.64[o]	0.60[s]	0.04	−0.14[o]	0.78	−0.21	0.85
3.35	7	1	0.77[m]	0.65[m]	0.12	−0.19[m]	0.96	−0.21	0.98
1.90	60	100	−0.23[s]	—	—	—	—	—	—
2.51	47	78	0.26[s]	−0.03[s]	0.29	—	—	−1.86	2.12
2.72	33	55	0.66[s]	−0.07[s]	0.73	—	—	−1.24	1.90
3.24	7	12	0.89[s]	−0.39[s]	1.28	—	—	−0.34	1.23
3.54	2.7	4.5	1.00[s]	−0.46[s]	1.46	—	—	−0.26	1.26

Dash indicates value not determined. Superscripts on measured Fe isotope values indicate technique: m, Menlo Park TIMS; o, Orleans Neptune multi-collector ICPMS; s, UC Santa Cruz Neptune multi-collector ICPMS. pH values are those of initial solution mixture prior to formation of precipitate. Fe concentrations of solutions were measured after formation of precipitate for 5 min.

[a] Measured values.

[b] Total precipitate calculated by mass balance assuming concentration and Fe isotope composition of $Fe[II]_{aq}$ are correct.

[c] Fractionation factor based on calculated total precipitate.

Table 5
Ferric chloride and ferric sulfate precipitation experiments (long-term)

Sample time	pH	Fe_{aq} (ppm)	$\delta^{56}Fe_{aq}$[a]	$\delta^{56}Fe_{ppt}$[a]	$\Delta^{56}Fe_{aq\text{-}ppt}$
Fe[III]Cl₃					
Time = 0 min	2.50	600.00	−0.22[o]	—	—
30 min	2.50	420.00	−0.05[o]	−0.65[o]	0.60
24 h	2.45	430.00	0.00[o]	−0.60[o]	0.60
1 week	2.46	410.00	0.20[o]	−0.66[o]	0.86
2 weeks	2.43	400.00	0.18[o]	−0.80[o]	0.98
Fe[III]₂(SO₄)₃					
Time = 0 min	2.66	465.00	−0.19[o]	—	—
30 min	2.66	320.00	0.06[o]	−0.52[o]	0.58
24 h	2.60	300.00	−0.01[o]	−0.67[o]	0.66
1 week	2.46	320.00	0.09[o]	−0.60[o]	0.69

Dash indicates value not determined. Superscripts on measured Fe isotope values indicate technique: o, Orleans Neptune multi-collector ICPMS. pH values are those of initial solution mixture prior to formation of precipitate. Fe concentrations of solutions were measured after formation of precipitate for the given time period.

[a] Measured values.

>0.8 μm fraction. The results suggest that iron isotope fractionation associated with solid precipitation can be expressed in both size fractions, and the pH/rate effect is consistently expressed during the formation of smaller, colloidal Fe(III)-oxyhydroxides, but may also be expressed during re-crystallization and precipitation of larger-sized Fe(III)-oxyhydroxides in some systems (e.g., $FeCl_3$).

In the short-term experiments at given pH/rate, $\Delta^{56}Fe_{aq\text{-}ppt}$ in the sulfate system was consistently greater than that in the chloride system (Table 4; Fig. 3), suggesting different importance of factors such as anion ligand effects preceding precipitation, solid–liquid boundary layer dynamics or within-solid diffusional gradients leading to kinetic isotope effects. Mineralogy of the precipitates may also play a role in the observed differences between the chloride and sulfate systems, as X-ray diffraction studies of the precipitates revealed that the sulfate solutions precipitated schwertmannite while the chloride solutions precipitated akaganeite. In addition, at given pH/rate in both the sulfate and chloride systems $\Delta^{56}Fe_{aq\text{-}ppt}$ was greater in the experiments carried out at lower concentrations (Table 4; Fig. 3). This apparent concentration effect may result from differences in diffusional gradients at the mineral–liquid interface in the low- and high-concentration experiments.

Table 6
Calculated percent aqueous species for ferric iron precipitation experiments

Ferric sulfate	$[Fe]^{3+}$	$[Fe(OH)]^{2+}$	$[Fe(OH)_2]^{+}$	$[FeSO_4]^{+}$	$[Fe(SO_4)_2]^{-}$	$[FeHSO_4]^{2+}$
High concentration						
Short: pH 1.90	9.65	0.28	0.00	81.69	4.47	3.90
Short: pH 3.35	5.05	4.51	0.20	82.87	7.21	0.16
Long: pH 2.46	8.12	0.95	0.01	85.50	4.26	1.17
Low concentration						
Short: pH 1.90	34.83	1.19	0.00	60.74	0.43	2.79
Short: pH 3.54	4.68	6.54	0.44	80.70	7.52	0.10
Ferric chloride	$[Fe]^{3+}$	$[Fe(OH)]^{2+}$	$[Fe(OH)_2]^{+}$	$[Fe_3(OH)_4]^{5+}$	$[FeCl]^{2+}$	$[FeCl_2]^{+}$
High concentration						
Short: pH 1.90	69.83	1.89	0.00	0.00	26.73	1.55
Short: pH 3.22	44.56	33.63	0.75	0.69	19.10	1.26
Long: pH 2.46	66.03	7.01	0.03	0.00	25.41	1.50
Low concentration						
Short: pH 1.90	91.00	2.98	0.01	0.00	5.96	0.06
Short: pH 3.53	35.15	57.17	4.86	0.05	2.74	0.03

Because $\Delta^{56}Fe_{aq\text{-}ppt}$ is consistently positive, one interpretation of the data is that a kinetic isotope effect is expressed during formation of the solid due to the inability of iron in freshly formed material at the solid–liquid interface to back-react with iron in solution. In order to determine if the apparent kinetic isotope effect might be reduced with lesser precipitation rates, longer-term (2–3 weeks) precipitation experiments were conducted. As shown in Fig. 3, the data for both the sulfate and chloride systems in these long-term experiments describe a single trend of decreasing $\Delta^{56}Fe_{aq\text{-}ppt}$ with increasing precipitation rate that has a much shallower slope than the general trend described by the data for the short-term experiments. The data can be interpreted to indicate a closer approach to and perhaps attainment of equilibrium in the long-term experiments. Given this perspective, short-term precipitation in both the sulfate and chloride systems apparently produces Fe(III) oxyhydroxides that are not in isotopic equilibrium with their host solutions, but with increased contact and/or aging of solid, equilibrium may be approached in each system.

4. Discussion

4.1. Isotopic fractionation between $Fe(II)_{aq}$ and $Fe(III)_{aq}$

In our experiments, net isotopic fractionations between the $Fe(II)_{aq}$, $Fe(III)_{aq}$, and $Fe(III)_{ppt}$ pools were determined by three competing processes: oxidation of $Fe(II)_{aq}$, isotopic equilibrium via electron transfer between $Fe(II)_{aq}$ and $Fe(III)_{aq}$, and precipitation of $Fe(III)_{aq}$ as either schwertmannite or akaganeite. The fundamental basis of the study design was to set up experiments in which oxidation of Fe(II) was driven by microbial activity. For a biological effect to be expressed in the Fe(III) products, that effect would have to overwhelm the non-biological equilibration and precipitation effects. As noted above, Johnson et al. (2002) and Welch et al. (2003) determined that the time required to reach isotopic equilibrium between $Fe(III)_{aq}$ and $Fe(II)_{aq}$ at pH 2.5 was ~1 min at 22 °C and they modeled the process as a second-order reaction with rate constant ~0.2 s^{-1} (~17,000 day^{-1}). In their experimental system, the principal aqueous species were $[Fe(II)(H_2O)_6]^{2+}$ (>97% of $Fe(II)_{aq}$ species), and $[Fe(III)(H_2O)_6]^{3+}$ and $[Fe(III)(H_2O)_5(OH)]^{2+}$ (>90% of $Fe(III)_{aq}$ species). Thus, one might have initially predicted that given the anticipated slow rates of microbial Fe(II) oxidation (rate constant ~0.01–0.03 day^{-1} for our experiments; Fig. 1), equilibrium between $Fe(II)_{aq}$ and $Fe(III)_{aq}$ should have been the dominant control on isotopic distribution among aqueous species. However, it was not possible a priori to rule out a biological control on $Fe(III)_{aq}$ chemistry (e.g., strong Fe(III)-ligand formation) that might have hindered or prevented backreaction of the $Fe(III)_{aq}$ pool with the remaining $Fe(II)_{aq}$ pool and/or modified the kinetics of solid-phase precipitation.

In fact, if only the $Fe(II)_{aq}$ data for the biological experiments are considered, then a reasonable interpretation of our data would be that isotopic distribution during the microbial oxidation process was governed by a Rayleigh mechanism having $\varepsilon \sim 2.2‰$ (Fig. 2A). This value is substantially less than the 2.9‰ value determined by Johnson et al. (2002) and Welch et al. (2003) for isotopic equilibrium between $[Fe(II)(H_2O)_6]^{2+}$ and $[Fe(III)(H_2O)_{6-x}(OH)_x]^{(3-x)+}$, and could be interpreted as reflecting a biological control on the isotopic distribution. Croal et al. (2004), in a study of iron isotope fractionation by Fe(II)-oxidizing photoautotrophic bacteria, obtained broadly similar results to ours in that the isotopic contrast between their hydrous Fe(III)-precipitates and $Fe(II)_{aq}$ was ~1.5‰ (compare with Table 3) and the evolution of $\delta^{56}Fe(II)_{aq}$ in their two experiments using different enrichment cultures was consistent with control by a Rayleigh mechanism having $\varepsilon \sim 1.1$ and 1.8‰, respectively. They concluded that the observed fractionation between $Fe(III)_{ppt}$ and $Fe(II)_{aq}$ was controlled either by

overprinting of isotopic equilibrium between Fe(II)- and Fe(III)-hexaquo/hydroxyl species by a kinetic isotope effect associated with formation of the $Fe(III)_{ppt}$ pool or by formation of "biological ligands" that established a different isotopic equilibrium between $Fe(II)_{aq}$ and $Fe(III)_{aq}$ pools. However, in the absence of measurements of the isotopic composition of the $Fe(III)_{aq}$ fraction that was difficult to isolate given the circum-neutral pH conditions of their experiments, it was not possible to decide between these contrasting mechanisms.

By determining the iron isotope composition of the $Fe(III)_{aq}$ products of our biological experiments, we are able to better constrain the actual fractionation between the $Fe(II)_{aq}$ and $Fe(III)_{aq}$ pools. As shown in Fig. 2B, the data for aqueous iron are generally well described by an equilibrium mechanism between $Fe(II)_{aq}$ and $Fe(III)_{aq}$ having $\varepsilon \sim 2.9‰$, consistent with the experimental work of Johnson et al. (2002) and Welch et al. (2003). We note that there is considerable scatter to the data, and a few of the data are significantly displaced from the equilibrium model curves. As pointed out by Johnson et al. (2002), the potential impact of progressive re-equilibration of the $Fe(II)_{aq}$ and $Fe(III)_{aq}$ pools during formation of a ferric iron precipitate must be evaluated. Moreover, it is worthwhile to consider additional mechanisms that may contribute to the data scatter.

Assuming that $Fe(II)_{aq}$ and $Fe(III)_{aq}$ pools were in isotopic equilibrium prior to addition of NaOH to promote rapid precipitation of the $Fe(III)_{aq}$ pool, isotopic re-equilibration would have occurred only if $\Delta^{56}Fe(III)_{aq\text{-}ppt}$ was different from 0‰ during the precipitation process (i.e., if the isotopic contrast between $Fe(II)_{aq}$ and $Fe(III)_{aq}$ progressively changed due to precipitation of a solid having different δ^{56}Fe than $Fe(III)_{aq}$). Considering the results of our Fe(III) precipitation experiments (Fig. 3), however, it is likely that $\Delta^{56}Fe(III)_{aq\text{-}ppt}$ was close to 0‰ given the rapidity of the precipitation process (i.e., on the order of seconds). Johnson et al. (2002) found no significant isotopic fractionation between $Fe(III)_{aq}$ and Fe(III)-oxyhydroxide precipitated over a period of a few seconds. Although these workers did correct the isotope compositions obtained in their exchange experiments using isotopically enriched iron for the effects of re-equilibration, they concluded that it was not necessary to do so for their exchange experiments using "normal" iron. Regardless, given that $\Delta^{56}Fe(III)_{aq\text{-}ppt}$ was consistently positive in our Fe(III) precipitation experiments, re-equilibration in our experimental system can only decrease the isotopic contrast between $Fe(II)_{aq}$ and $Fe(III)_{aq}$ pools, and thus the average measured contrast of ~2.9‰ is a minimum.

The significant displacement of a few data points from the equilibrium model curves in Fig. 2 points to an additional process that overprints apparent isotope equilibrium between $Fe(II)_{aq}$ and $Fe(III)_{aq}$ pools. In the most extreme cases, the $\delta^{56}Fe(III)_{aq}$ value lies above the $Fe(III)_{aq}$ model curve in Fig. 2B while the corresponding $\delta^{56}Fe(II)_{aq}$ value lies below the $Fe(II)_{aq}$ model curve. In addition, these offsets from the equilibrium model curves appear to reflect isotope mass balance, such that when the concentration of $Fe(II)_{aq}$ is greater than that of $Fe(III)_{aq}$ (i.e., early in each experiment), $\delta^{56}Fe(III)_{aq}$ is further displaced from the equilibrium curve than $\delta^{56}Fe(II)_{aq}$. Such offsets are consistent with enhanced sorption of Fe(II) on the $Fe(III)_{ppt}$ substrate. Icopini et al. (2004) and Johnson et al. (2005) demonstrated that Fe(II) preferentially sorbed to rapidly forming hydrous ferric oxide substrates may have δ^{56}Fe more than 2‰ greater than that of the bulk $Fe(II)_{aq}$ pool. Note that our procedure to correct the measured $\delta^{56}Fe(II)_{aq}$ and $\delta^{56}Fe(III)_{aq}$ values (Section 3.1) assumes that the Fe(II) component of the operational $Fe(III)_{aq}$ pool has δ^{56}Fe identical to that of the $Fe(II)_{aq}$ pool. Substituting a greater value for "$\delta^{56}Fe(II)_{aq}$" in the first term of Eq. (2) results in a lesser calculated value for $\delta^{56}Fe(III)_{aq}$ and a greater calculated value for $\delta^{56}Fe(II)_{aq}$, and moves the data points closer to the equilibrium model curves. It is unclear, however, why some samples would have been more prone than others to such a sorption effect, and there may be other explanations for the observed offsets.

The overall similarity of the data array to the equilibrium model curves suggests that isotopic equilibration between $Fe(II)_{aq}$ and $Fe(III)_{aq}$ due to electron transfer dominates any isotopic effects associated with microbial Fe(II) oxidation or Fe(III) precipitation. Further, this result suggests that equilibration between $[Fe(II)(H_2O)_6]^{2+}$ and $[Fe(III)(H_2O)_{6-x}(OH)_x]^{(3-x)+}$ aqueous species was the dominant control on isotopic fractionation between the $Fe(II)_{aq}$ and $Fe(III)_{aq}$ pools, as in the experiments of Johnson et al. (2002) and Welch et al. (2003). Finally, as shown in Fig. 4, the $Fe(II)_{aq}$ data of Croal et al. (2004) cluster with the data from our biological experiments, suggesting that a similar interpretation of their experimental results is reasonable. However, in order to confirm this interpretation, it will be necessary to develop novel and clever techniques with which to actually determine the iron isotope composition of the minor $Fe(III)_{aq}$ pool formed at

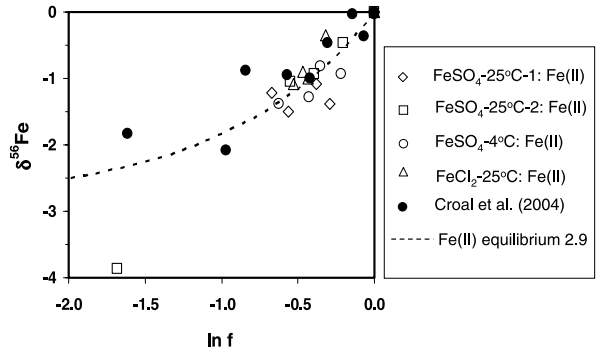

Fig. 4. δ^{56}Fe of corrected $Fe(II)_{aq}$ components for all biological oxidation experiments, plotted against $\ln(f)$, where f is the proportion of $Fe(II)_{aq}$ remaining. Data from experiments of Croal et al. (2004) are included for comparison. Data are plotted relative to starting material for each experiment, where the initial value is taken to be 0‰. Dashed line represents the equilibrium fractionation trend having isotopic enrichment factor $\varepsilon = 2.9‰$.

the circum-neutral pH conditions used in the experiments of Croal et al. (2004).

4.2. Isotopic fractionation associated with $Fe(III)_{aq}$ precipitation

To interpret isotopic fractionation between $Fe(II)_{aq}$ and Fe(III)-oxyhydroxides properly, an important goal of our study was to assess causes of isotopic fractionation between $Fe(III)_{aq}$ and Fe(III)-oxyhydroxide during Fe(III) precipitation. In our Fe(III) precipitation experiments (Table 4; Fig. 3), a range of pHs were used in order to investigate the possible effects of precipitation rate on fractionation. In these experiments, pH was adjusted in order to vary precipitation rate. However, recent work on carbonates by Adkins et al. (2003) contested the use of pH as a proxy for precipitation rate and maintained that isotope effects associated with changes in pH are a function of changes in speciation among ionic components containing the isotopes in question. In order to examine possible controls of iron aqueous speciation on isotope fractionation in the precipitation experiments, we have calculated the Fe(III) aqueous species distribution for several of the short- and long-term experimental solutions for both the sulfate and chloride systems, using the WATEQ4f speciation code (Ball and Nordstrom, 1991). The results are listed in Table 6.

Variations in iron aqueous speciation with changing pH appear to have little relation to the fractionation observed in our experiments. For example, over the pH range of the short- and long-term high-concentration experiments with ferric sulfate, the relative proportions of Fe aqueous species changed little, yet $\Delta^{56}Fe_{aq\text{-}ppt}$ varied by $\sim$1‰. In contrast, over the same pH range in the short-term low-concentration experiments with ferric sulfate, the relative proportions of iron aqueous species changed considerably (particularly the ratio of aquo- to sulfate species), yet $\Delta^{56}Fe_{aq\text{-}ppt}$ varied by a similar amount. Moreover, over the pH range of the short-term low-concentration experiments with ferric chloride, concentrations of iron aqueous species changed considerably, yet $\Delta^{56}Fe_{aq\text{-}ppt}$ was essentially constant. Lacking a clear systematic correlation of isotopic contrast with aqueous speciation and given the systematic variation of $\Delta^{56}Fe_{aq\text{-}ppt}$ with our estimate of precipitation rate, we contend that the isotopic changes seen during these experiments are more likely related to the rate at which the precipitates formed.

In our precipitation experiments, we observed that $\Delta^{56}Fe_{aq\text{-}ppt}$ generally decreased from a positive value toward zero with increasing precipitation rate. Lack of isotopic fractionation at the greatest precipitation rates is consistent with the observations of Johnson et al. (2002), who developed a rapid precipitation technique to physically separate isotopically enriched $Fe(III)_{aq}$ from a $Fe(II)_{aq}$–$Fe(III)_{aq}$ mixture and found no isotopic contrast between the aqueous and solid products. However, decreasing $\Delta^{56}Fe_{aq\text{-}ppt}$ with increasing precipitation rate is seemingly at odds with the conclusions of Skulan et al. (2002), who observed increasing $\Delta^{56}Fe_{aq\text{-}ppt}$ with increasing precipitation rate during experimental precipitation of hematite. This apparent contradiction is likely related to the time scale and kinetics of the various experiments. Our lowest-pH experiments may be most analogous to the "rapid" hematite precipitation experiments of Skulan et al. (2002) that occurred over a 12-h timeframe. At precipitation rates corresponding to this time scale, kinetic isotope effects are perhaps controlled by diffusion gradients in the growing solid (cf. Gussone et al., 2003) and result in positive $\Delta^{56}Fe_{aq\text{-}ppt}$ values. At greater precipitation rates (e.g., in our high-pH experiments and in the Johnson et al. (2002) "rapid precipitation" experiment), diffusion gradients in the liquid immediately adjacent to the growing solid may limit the ability of residual, isotopically heavy $Fe(III)_{aq}$ in this liquid boundary layer to isotopically equilibrate with the remaining $Fe(III)_{aq}$ pool. Progressive precipitation under this condition would result in $\Delta^{56}Fe_{aq\text{-}ppt}$ approaching 0‰. At lesser precipitation rates (e.g., the 200-day "equilibrium" experiment of Skulan et al., 2002), there would be the greatest potential for true isotopic equilibrium between solid and liquid. Given this perspective, the overall lesser $\Delta^{56}Fe_{aq\text{-}ppt}$ values in our long-term experiments compared to those in the short-term experiments could be interpreted as reflecting a closer approach to equilibrium, perhaps due to longer contact time between mineral surface and liquid prior to armoring of the surface by subsequently precipitated material. If precipitation rate in our long-term experiment could have been slowed even further (e.g., by conducting the experiment at slightly lower pH), the slope of the resulting trend in Fig. 3 might have approached zero.

Although it is clear from our experiments that different reaction times at a given pH result in different $\Delta^{56}Fe_{aq\text{-}ppt}$, it remains unclear whether equilibrium values of $\Delta^{56}Fe_{aq\text{-}ppt}$ are in the 0.7–0.9‰ range for the ferric sulfate and chloride systems as measured in our long-term experiments or are closer to 0‰ as observed by Skulan et al. (2002) for the ferric oxide system. Regardless, in order for equilibrium effects to be expressed, slow rates of precipitation apparently are required. This is supported by the theoretical work of Watson (2004) who looked at near-surface kinetic controls on the isotopic composition of carbonates. Watson's (2004) model predicts that during rapid precipitation of carbonate, the surface of the precipitating crystal represents a reaction front that can have an isotopic composition that is not at equilibrium with that of the surrounding water, depending primarily on the isotopic equilibration rate that is largely diffusion limited. If the precipitation rate exceeds the isotopic equilibration rate, this non-equilibrium isotopic signature will be incorporated into the mineral.

The differences in $\Delta^{56}Fe_{aq\text{-}ppt}$ of the different size fractions in our precipitation experiments apparently support such a model. In those experiments, the smaller size fraction (0.1–0.8 μm) is intermediate in isotopic composition between that of the >0.8 μm and $Fe(III)_{aq}$ fractions, and tends to be significantly higher (by as much as $\sim$1.0‰) than

the >0.8 μm fraction. The 0.1–0.8 μm fraction may be associated with earlier and/or faster rates of precipitation and might reflect the isotopic composition of a colloidal intermediate, while the >0.8 μm fraction may be associated with later and/or slower rates of precipitation. With time, amalgamation and dissolution/re-crystallization occurs and larger Fe(III)-oxyhydroxide precipitates form. At the slowest rates of precipitation, the net isotopic fractionation observed may be the additive fractionation effects associated with the formation of each size fraction, depending primarily on the ability of early-formed solids to re-equilibrate with the evolving $Fe(III)_{aq}$ pool. If true, this suggests that multiple rate-controlling steps occur during slower Fe(III) precipitation at lower pH and the fractionation effects of each step may be expressed in the final product.

Dependence of $\Delta^{56}Fe(III)_{aq\text{-}ppt}$ on precipitation rate may help to explain the variability of $\Delta^{56}Fe(III)_{aq\text{-}ppt}$ observed in our biological experiments. In all biological experiments conducted at 25 °C, $\Delta^{56}Fe(III)_{aq\text{-}ppt}$ is greatest in the earlier stages and least in the later stages of Fe(II) oxidation (Table 3). Precipitation of Fe(III)-oxyhydroxide is presumably a first-order reaction (Beard and Johnson, 2004), and thus precipitation rate should correlate with $Fe(III)_{aq}$. Thus, in the earlier stages of Fe(II) oxidation when $Fe(III)_{aq}$ concentrations are low, the precipitation rate should be correspondingly slow and $\Delta^{56}Fe(III)_{aq\text{-}ppt}$ should be greatest. As $Fe(III)_{aq}$ concentrations increase with protracted Fe(II) oxidation, the precipitation rate should increase and $\Delta^{56}Fe(III)_{aq\text{-}ppt}$ should decrease toward 0‰. However, although simple precipitation rate considerations can account for the results of the experiments conducted at 25 °C, the results of the experiment using ferrous sulfate at 4 °C argue for additional controls. In that experiment, $\Delta^{56}Fe(III)_{aq\text{-}ppt}$ actually increased through the 56-day time point, then decreased to a negative value by the 70-day time point (Table 3). Although one can speculate about unique kinetics associated with precipitation of Fe(III)-oxyhydroxides in this low-temperature condition, there is little hard evidence that can be used to account for this different behavior. Furthermore, abiotic controls prepared at 4 °C resulted in no measurable oxidation and thus offer no additional interpretive insight.

4.3. Implications

An important conclusion of this study is that any characteristic iron isotope fractionation directly related to relatively slow microbial oxidation of Fe(II) that might constitute a "biosignature" is likely to be overprinted by relatively rapid isotopic equilibration between $Fe(II)_{aq}$ and $Fe(III)_{aq}$ pools. Thus, it is unlikely that such a biosignature would be expressed in the geologic record. Furthermore, it is likely that isotopic fractionation between coexisting Fe(II)- and Fe(III)-minerals will largely reflect the extent of overprinting of the equilibrium fractionation by kinetic fractionation during mineral precipitation. We suggest that $\Delta^{56}Fe_{Fe(III)\text{-}Fe(II)}$ for coexisting Fe(III)- and Fe(II)-minerals should approach +3‰ when $Fe(II)_{aq}$ and $Fe(III)_{aq}$ are in isotopic equilibrium and kinetic effects associated with Fe(III) precipitation are minimal (i.e., when Fe(III) precipitation rates are either extremely fast or extremely slow).

For example, Rouxel et al. (2005) reported $\delta^{56}Fe$ values of contemporaneous Archaen to Paleoproterozoic pyrites in black shales and iron oxides separated from banded iron formations. A maximum difference of ~3‰ in the $\delta^{56}Fe$ values of these minerals was observed during the period from 2.8 to 2.3 Ga, prior to the presumed rise of atmospheric oxygen. This extent of fractionation is consistent with isotopic equilibrium between $Fe(II)_{aq}$ and $Fe(III)_{aq}$ in the oceans at that time and considerable oxidation of the original $Fe(II)_{aq}$ pool in order to drive $\delta^{56}Fe$ values of Fe(II) in pyrite to less than -2‰. This of course assumes that mineral precipitation rates were either extremely rapid or extremely slow such that kinetic isotope effects were not expressed in the minerals. Regardless, even if microbial activity were important to the formation of the iron pools from which these minerals precipitated, it would be difficult to identify an iron isotope biosignature component due to overprinting by the abiotic processes.

The results of this study demonstrate, at least for low-pH environments, the importance of aqueous redox chemistry in controlling iron isotope fractionation that can be recorded in mineral products. Furthermore, the ranges of fractionation between $Fe(II)_{aq}$ and $Fe(III)_{ppt}$ pools observed during oxidation of Fe(II) by aerobic acidophilic bacteria (the present study), oxidation of Fe(II) by anaerobic photoautotrophic bacteria (Croal et al., 2004) and dissimilatory reduction of Fe(III) substrates by either strict or facultative anaerobic bacteria (Beard et al., 2003) are similar to that observed during abiotic oxidation of Fe(II) in the presence of oxygen at circum-neutral pH (Bullen et al., 2001). Thus, unless it is possible to unambiguously establish that anoxygenic conditions persisted in the depositional environment of any particular iron–mineral pair in the rock record, it appears that iron isotopes on their own will not provide a diagnostic biosignature tool. However, as pointed out by Johnson et al. (2004), establishment of coexisting $Fe(II)_{aq}$ and $Fe(III)_{aq}$ pools, and thus an isotope fractionation mechanism, in the absence of free oxygen during early earth history could have been accomplished through anaerobic oxidation of $Fe(II)_{aq}$ by photoautotrophic bacteria. In this case, the resulting isotope fractionation between coexisting Fe(II)- and Fe(III)-minerals might constitute a true biosignature. Although a promising prospect, it remains necessary and challenging to demonstrate that such mineral pairs are primary, and that other abiotic processes such as open-system sorption of Fe(II) on secondary minerals such as clays (cf. Icopini et al., 2004) did not constitute effective alternative isotope fractionation mechanisms that could have promoted development of isotopically diverse $Fe(II)_{aq}$ pools.

Finally, the consistency of iron isotope fractionation between $Fe(III)_{ppt}$ and $Fe(II)_{aq}$ (i.e., $\Delta^{56}Fe_{Fe(III)ppt\text{-}Fe(II)aq}$) observed during oxidation of ferrous iron, either through microbial activity (e.g., Croal et al., 2004; this study) or by reaction with oxygen at circum-neutral pH (e.g., Bullen et al., 2001), could imply a common isotope fractionation mechanism. Certainly, the fact that $\Delta^{56}Fe_{Fe(III)ppt\text{-}Fe(II)aq}$ in all these situations is <3‰ begs a model in which isotopic equilibrium established between $Fe(II)_{aq}$ and $Fe(III)_{aq}$ pools is overprinted by kinetic effects associated with the solid precipitation step. Welch et al. (2003) and Beard and Johnson (2004) invoked such a model to explain isotope fractionation observed by Bullen et al. (2001) in laboratory and field studies of abiotic iron oxidation.

However, although such a model elegantly explains iron isotope fractionation observed in the microbial experiments conducted at very slow Fe(II) oxidation rates, it fails to explain key aspects of the results reported by Bullen et al. (2001) for faster Fe(II) oxidation rates. In particular, the extremely short residence time of $Fe(III)_{aq}$ (~seconds) and high $Fe(II)_{aq}/Fe(III)_{aq}$ ratios (>1000) characterizing these field and laboratory studies allow at best only a partial approach to isotopic equilibrium between $Fe(II)_{aq}$ and $Fe(III)_{aq}$ pools, given the ~60-s timeframe for establishment of isotopic equilibrium between the $[Fe(II)(H_2O)_6]^{2+}$ and $[Fe(III)(H_2O)_{6-x}(OH)_x]^{(3-x)+}$ aqueous species documented by Johnson et al. (2002) and Welch et al. (2003). Moreover, using the results of our Fe(III) precipitation experiments as a guide, we suggest that the extremely rapid ferric oxyhydroxide precipitation rates typical of well oxygenated, circum-neutral pH conditions should prevent kinetic isotope effects from being expressed in the solid products. Indeed, Welch et al. (2003) point out that "previous experiments in our (University of Wisconsin) laboratory (e.g., Johnson et al., 2002; Skulan et al., 2002) have demonstrated that extremely rapid precipitation (~seconds) produces no significant isotopic fractionation between Fe(II) in solution and the ferric-oxyhydroxide precipitates (~0.2‰ uncertainty)."

Apparently there are other controls on the observed isotopic contrast between $Fe(II)_{aq}$ and $Fe(III)_{ppt}$ pools produced under well-oxygenated, circum-neutral pH conditions. Bullen et al. (2001) stressed the importance of oxidation through the ferrous hydroxyl pathway, and suggested that an aqueous complex along that pathway could be isotopically heavy relative to the bulk $Fe(II)_{aq}$ pool, thus promoting an isotopically heavy $Fe(III)_{aq}$ pool. An intriguing alternative is that increased importance of electron transfer and isotopic equilibrium between the highly reactive ferrous and ferric hydroxyl aqueous complexes with increasing pH may hasten isotopic equilibration, likewise promoting an isotopically heavy $Fe(III)_{aq}$ pool even at high rates of iron flux through that pool. Clearly more work is needed to fully understand iron isotope fractionation mechanisms under these conditions.

5. Conclusions

This is the first study to measure the iron isotope distribution between $Fe(II)_{aq}$, $Fe(III)_{aq}$, and $Fe(III)_{ppt}$ during bacterial and abiotic Fe(II) oxidation in ferrous sulfate and ferrous chloride solutions at low-pH conditions that might be typical of acid mine drainage. Although the original purpose of this study was to determine the impact of biological processes on the iron isotope composition of the ferric iron products of oxidation, our main conclusion is that the isotopic distribution was controlled by abiotic processes. Using a novel method to separate the product $Fe(III)_{aq}$ from residual $Fe(II)_{aq}$ following oxidation over varying reaction times, we found that both $\delta^{56}Fe(III)_{aq}$ and $\delta^{56}Fe(III)_{ppt}$ were consistently greater than $\delta^{56}Fe(II)_{aq}$, and that overall the aqueous data are well explained by an isotopic equilibrium model having $\varepsilon = 2.9‰$. This fractionation factor is identical to that established previously for isotopic equilibrium between $Fe(II)_{aq}$ and $Fe(III)_{aq}$ due to electron transfer. Our results argue against control by "biological ligands" that could hinder or prevent isotopic equilibration between $[Fe(II)(H_2O)_6]^{2+}$ and $[Fe(III)(H_2O)_{6-x}(OH)_x]^{(3-x)+}$ aqueous species, and thus impart a biological signature on the ferric iron products of oxidation. In a series of abiotic experiments in which schwertmannite or akaganeite were precipitated from ferric sulfate and ferric chloride solutions, respectively, we found that $\delta^{56}Fe(III)_{aq}$ was generally similar to or greater than $\delta^{56}Fe(III)_{ppt}$, and that $\Delta^{56}Fe(III)_{aq\text{-}ppt}$ depended largely on rate of precipitation. Fractionation between $Fe(III)_{aq}$ and $Fe(III)_{ppt}$ pools was substantially greater in the sulfate system compared to that in the chloride system, perhaps due to differences in ligand formation prior to precipitation, or to greater diffusion limitation either at the solid–liquid interface or within precipitates in the sulfate system compared to that in the chloride system.

Acknowledgments

We thank Ariel Anbar, Clark Johnson, and an anonymous reviewer for their helpful and challenging comments on this manuscript. In addition, we thank John Fitzpatrick for assistance during sample preparation, and Jugdeep Aggarwal for assistance during isotope analysis on the Neptune instrument at UC Santa Cruz. This work was supported by a National Science Foundation Career grant to K.W.M. (EAR-9985234).

Associate editor: Donald E. Canfield

References

Adkins, J.F., Boyle, E.A., Curry, W.B., Lutringer, A., 2003. Stable isotopes in deep-sea corals and a new mechanism for "vital effects". *Geochim. Cosmochim. Acta* **67**, 1129–1143.

Anbar, A.D., Roe, J.E., Barling, J., Nealson, K.H., 2000. Nonbiological fractionation of iron isotopes. *Science* **288**, 126–128.

Anbar, A.D., 2004. Iron stable isotopes: beyond biosignatures. *ESPL Frontiers* **217**, 223–236.

Anbar, A.D., Jarzecki, A.A., Spiro, T.G., 2005. Theoretical investigation of iron isotope fractionation between $Fe(H_2O)_6^{3+}$ and $Fe(H_2O)_6^{2+}$: implications for iron stable isotope geochemistry. *Geochim. Cosmochim. Acta* **69**, 825–837.

Arnold, G.L., Weyer, S., Anbar, A.D., 2004. Fe isotope variations in natural materials measured using high mass resolution multiple collector ICPMS. *Anal. Chem.* **76**, 322–327.

Ball, J.W., Nordstrom, D.K., 1991. WATEQ4f—User's manual with revised thermodynamic data base and test cases for calculating speciation of major, trace and redox elements in natural waters. *U.S. Geological Survey Open-File Report* **91-183**, 185.

Beard, B.L., Johnson, C.M., Cox, L., Sun, H., Nealson, K.H., Aguilar, C., 1999. Iron isotope biosignatures. *Science* **285**, 1889–1892.

Beard, B.L., Johnson, C.M., Skulan, J.L., Nealson, K.H., Cox, L., Sun, H., 2003. Application of Fe isotopes to tracing the geochemical and biological cycling of Fe. *Chem. Geol.* **195**, 87–117.

Beard, B.L., Johnson, C.M., 2004. Fe isotope variations in the modern and ancient earth and other planetary bodies. *Rev. Mineral. Geochem.* **55**, 319–357.

Bigham, J.M., Schwertmann, U., Carlson, L., Murad, E., 1990. A poorly crystallized oxyhydroxysulfate of iron formed by bacterial oxidation of Fe(II) in acid mine waters. *Geochim. Cosmochim. Acta* **54**, 2743–2758.

Brett, J.B., Banfield, J., 2003. Microbial communities in acid mine drainage. *FEMS Microbiol. Ecol.* **44**, 139–152.

Blowes, D.W., Ptacek, C.J., Jurjovec, J., 2003. Mill Tailings: hydrogeology and geochemistry. In: Jambor, J.L., Blowes, D.W., Ritchie, A.I.M. (Eds.), *Environmental Aspects of Mine Wastes*. Short Course series **31**, 95–116.

Bullen, T.D., White, A., Childs, C.W., Vivit, D.V., Schulz, M., 2001. Demonstration of significant abiotic iron isotope fractionation in nature. *Geology* **29**, 699–702.

Croal, L.R., Johnson, C.M., Beard, B.L., Newman, D.K., 2004. Iron isotope fractionation by Fe(II)-oxidizing photoautotrophic bacteria. *Geochim. Cosmochim. Acta* **68**, 1227–1242.

Donati, E., Pogliani, C., Boiardi, J.L., 1997. Anaerobic leaching of covellite by *Thiobacillus ferrooxidans*. *Appl. Environ. Microbiol.* **47**, 636–639.

Ehrlich, H.L., 1996. *Geomicrobiolgy*, third ed. Marcel Dekker, New York, NY.

Ferris, F.G., Tazaki, K., Fyfe, W.S., 1989. Iron oxides in acid mine drainage environments and their association with bacteria. *Chem. Geol.* **74**, 321–330.

Fry, I.V., Lazaroff, N., Packer, L., 1986. Sulfate dependent iron oxidation by *T. ferrooxidans*: characterization of a new EPR detectable electron transport component on the reducing side of rusticyanin. *Arch. Biochem. Biophys.* **246**, 650–654.

Ghiorse, W.C., 1984. Biology of iron and manganese-depositing bacteria. *Annu. Rev. Microbiol.* **38**, 515–550.

Glasauer, S., Weidler, P.G., Langley, S., Beveridge, T.J., 2003. Controls on Fe reduction and mineral formation by a subsurface bacterium. *Geochim. Cosmochim. Acta* **67**, 1277–1288.

Gussone, N., Eisenhauer, A., Heuser, A., Dietzel, M., Bock, B., Bohm, F., Spero, H., Lea, D., Buma, J., Nagler, T.F., 2003. Model for kinetic effects on calcium isotope fractionation (δ^{44}Ca) in inorganic aragonite and cultured planktonic foraminifera. *Geochim. Cosmochim. Acta* **67**, 1375–1382.

Harahuc, L., Lizama, H.M., Suzuki, I., 2000. Selective inhibition of the oxidation of ferrous iron or sulfur in *Thiobacillus ferrooxidans*. *Appl. Environ. Microbiol.* **66**, 1031–1037.

Icopini, G.A., Anbar, A.D., Ruebush, S.S., Tien, M., Brantley, S.L., 2004. Iron isotope fractionation during microbial reduction of iron: the importance of adsorption. *Geology* **32**, 205–208.

Johnson, T.M., Bullen, T.D., Zawlislanski, P.T., 2000. Selenium stable isotope ratios as indicators of sources and cycling of selenium: results from the northern reach of San Francisco Bay. *Environ. Sci. Technol.* **34**, 2075–2079.

Johnson, C.M., Skulan, J.L., Beard, B.L., Sun, H., Nealson, K.H., Braterman, P.S., 2002. Isotopic fractionation between aqueous Fe(III) and Fe(II) in aqueous solutions. *Earth Planet. Sci. Lett.* **195**, 141–153.

Johnson, C.M., Roden, E.E., Welch, S.A., Beard, B.L., 2005. Experimental constraints on Fe isotope fractionation during magnetite and Fe carbonate formation coupled to dissimilatory hydrous ferric oxide reduction. *Geochim. Cosmochim. Acta* **69**, 963–993.

Jambor, J.L., 2003. Mine waste mineralogy and mineralogical perspective of acid–base counting. In: Jambor, J.L., Blowes, D.W., Ritchie, A.I.M. (Eds.), *Environmental Aspects of Mine Wastes*. Short Course series **31**, 117–145.

Kappler, A., Benz, M., Schink, B., Brune, A., 2004. Electron shuttling via humic acids in microbial iron(III) reduction in a freshwater sediment. *FEMS Microbiol. Ecol.* **47**, 85–92.

Lizama, H.M., Suzuki, I., 1989. Bacterial leaching of a sulfide ore by *Thiobacillus ferrooxidans* and *Thiobacillus thiooxidans* part II: column leaching studies. *Hydrometallurgy* **22**, 301–310.

Lovley, D.R., Phillips, E.J.P., 1986a. Organic matter mineralization with reduction of ferric iron in anaerobic sediments. *Appl. Environ. Microbiol.* **51**, 683–689.

Lovley, D.R., Phillips, E.J.P., 1986b. Availability of ferric iron for microbial reduction in bottom sediments of the freshwater tidal Potomac River. *Appl. Environ. Microbiol.* **52**, 751–757.

Lovley, D.R., Phillips, E.J.P., 1987. Rapid assay for microbially reducible ferric iron in aquatic sediment. *Appl. Environ. Microbiol.* **53**, 1536–1540.

Mandernack, K.W., Bazylinksi, D.A., Shanks, W.C., Bullen, T.D., 1999. Oxygen and iron isotope studies of magnetite produced by magnetotactic bacteria. *Science* **285**, 1892–1896.

Mariotti, A., German, J.C., Hubert, P., Kaiser, P., Letolle, R., Tardieux, A., Tardieux, P., 1981. Experimental determination of nitrogen kinetic isotope fractionation: some principles; illustration for denitrification and nitrification processes. *Plant Soil* **62**, 413–430.

Matthews, A., Zhu, X.K., O'Nions, K., 2001. Kinetic iron stable isotope fractionation between iron (-II) and (-III) complexes in solution. *Earth Planet. Sci. Lett.* **192**, 81–92.

Morgan, J.J., Stumm, W., 1998. Water properties. *Kirk–Othmer Encyclopedia of Chemical Technology*, fourth ed., vol. 25.

Nealson, K.H., Tebo, B.M., Rosson, R.A., 1988. Occurrence and mechanisms of microbial oxidation of manganese. *Adv. Appl. Microbiol.* **33**, 279–318.

Nordstrom, D.K., Southam, G., 1997. Geomicrobiology of sulfide mineral oxidation. In: Banfield, J.F., Nealson, K.H. (Eds.), *Geomicrobiology: Interactions between Microbes and Minerals*, vol. 35. Mineralogical Society of America, Washington, DC, pp. 361–390.

Roe, J.E., Anbar, A.D., Barling, J., 2003. Nonbiological fractionation of Fe isotopes: evidence of an equilibrium isotope effect. *Chem. Geol.* **195**, 69–85.

Rouxel, O.J., Bekker, A., Edwards, K.J., 2005. Iron isotope constraints on the Archean and Paleoproterozoic ocean redox state. *Science* **307**, 1088–1091.

Russell, W.A., Papanastassiou, D.A., Tombrello, T.A., 1978. Ca isotope fractionation on the Earth and other solar system materials. *Geochim. Cosmochim. Acta* **42**, 1075–1090.

Sampson, M.I., Phillips, C.V., Ball, A.S., 2000. Investigation of the attachment of *Thiobacillus ferrooxidans* to mineral sulfides using scanning electron microscopy analysis. *Miner. Eng.* **13**, 643–656.

Savic, D.S., Veljkovic, V.B., Lazic, M.L., Vrvic, M.M., Vucetic, J.I., 1998. Effects of the oxygen transfer rate on ferrous iron oxidation by *Thiobacillus ferrooxidans*. *Enzyme Microb. Technol.* **23**, 427–431.

Schauble, E.A., Rossman, G.R., TaylorJr, H.P., 2001. Theoretical estimates of equilibrium Fe-isotope fractionations from vibrational spectroscopy. *Geochim. Cosmochim. Acta* **65**, 2487–2497.

Schrenk, M., Edwards, K., Banfield, J., 1998. Distribution of *T. ferrooxidans* and *Leptospirillum ferrooxidans*: implication for generation of acid mine drainage. *Science* **279**, 1519–1521.

Schwertmann, U., Fitzpatrick, R.W., 1992. Iron minerals in surface environments. In: Skinner, H.C.W., Fitzpatrick, R.W. (Eds.), *Biomineralization: Processes of Iron and Manganese*. Cremlingen-Destadt, Germany, pp. 7–30.

Skulan, J.L., Beard, B.L., Johnson, C.M., 2002. Kinetic and equilibrium Fe isotope fractionation between aqueous Fe(III) and hematite. *Geochim. Cosmochim. Acta* **66**, 2995–3015.

Suzuki, I., 1999. Oxidation of inorganic sulfur compounds: chemical and enzymatic reactions. *Can. J. Microbiol.* **45**, 97–105.

Watson, E.B., 2004. A conceptual model for near-surface kinetic controls on the trace-element and stable isotope composition of abiogenic calcite crystals. *Geochim. Cosmochim. Acta* **68**, 1473–1488.

Welch, S.A., Beard, B.L., Johnson, C.M., Braterman, P.S., 2003. Kinetic and equilibrium Fe isotope fractionation between aqueous Fe(II) and Fe(III). *Geochim. Cosmochim. Acta* **67**, 4231–4250.

Weyer, S., Schwieters, J., 2003. High precision Fe isotope measurements with high mass resolution MC-ICP-MS. *Int. J. Mass Spectrom. Ion Process* **226**, 355–368.